INVESTIGATION OF COMPRESSOR CYCLE OPERATING POINT FOR VARIOUS AIR CONDITIONS

A Thesis Submitted to
the Graduate School of Engineering and Science of
İzmir Institute of Technology
in Partial Fulfillment of the Requirements for the Degree of

MASTER OF SCIENCE

in Mechanical Engineering

by
Soykan YAŞAR

October 2019

İZMİR

We approve the thesis of **Soykan YAŞAR**

Examining Committee Members:

Assoc. Prof. Dr. Erdal ÇETKİN
Department of Mechanical Engineering, İzmir Institute of Technology

Prof. Dr. Tahsin BAŞARAN
Department of Architecture, İzmir Institute of Technology

Prof. Dr. Aytunç EREK
Department of Mechanical Engineering, Dokuz Eylül University

7 October 2019

Assoc. Prof. Dr. Erdal ÇETKİN
Supervisor, Department of Mechanical Engineering, İzmir Institute of Technology

Prof. Dr. Sedat AKKURT
Head of the Department of Mechanical Engineering

Prof. Dr. Mehtap EANES
Dean of the Graduate School of Engineering and Science

ACKNOWLEDGMENTS

First of all, I would like to express my appreciation to my advisor Dr. Erdal ÇETKİN, for his guidance and help throughout this thesis.

I also would like to thank, I take this opportunity to express my gratitude to my family, Filiz, Serkan and Hikmet YASAR. They stood by me in every decision I made, gave me courage to step up, help me become the person I am.

Last but not least, I would like to thank my prospective partner, Gizem OZARKALIOGLU for her endless care, love and support.

ABSTRACT

INVESTIGATION OF COMPRESSOR CYCLE OPERATING POINT FOR VARIOUS AIR CONDITIONS

In this study, operating point of compression cycle for various conditions is documented with the consideration of all the equipment of vapor-compression refrigeration cycle. An algorithm which characterizes all the equipment, simulation of the cycle and enabling of the calculation of capacitive values is proposed. The algorithm includes compressor capacitive value polynomial coefficients, air and refrigerant side pressure drop and heat transfer correlations (for finned heat exchangers) which were taken from the literature to uncover the operating point and performance of each equipment in the cycle. e-Ntu and LMTD relations are discussed and proper correlations are included on the thesis. Furthermore, the mathematical models in the literature were surveyed in order to uncover circuiting analysis performed in the cycles.

Keywords and Phrases: HVAC, Compressor Cycle, Refrigeration, Heat exchanger

ÖZET

ÇEŞİTLİ HAVA KOŞULLARINDA KOMPRESÖR ÇEVİRİMİ ÇALIŞMA NOKTASININ ARAŞTIRILMASI

Bu çalışmada, buhar sıkıştırmalı kompresör çevrimi çalışma noktası, buhar sıkıştırmalı soğutma çevrimi ekipmanlarını kapsayacak şekilde incelenmiştir. İncelenen bu ekipmanların kapasitif hesaplamaların yapılabilmesi ve kompresör çevrimin similasyonunun gerçekleştirilebilmesi için algoritma mantığı araştırılmıştır. Kompresör kapasite hesaplarında polinom katsayıları, eşanjör yapılarında finli borulu eşanjörlerin hava ve akışkan tarafı ısı transfer ve basınç kaybı korelasyonları literatürden bulunmuştur. Isı transfer hesaplamaları için e-Ntu ve LMTD metodları üzerinde çalışılmış ve uygun korelasyonlar listelenmiştir. Bunun yanı sıra finli borulu eşanjörlerde matematiksel modeller, farklı devreleme şekillerine yönelik çevrim analizlerini gerçekleştirebilmek için irdelenmiştir.

Anahtar Kelimeler ve İfadeler: HVAC, Kompresör çevrimi, Soğutma, Isı değiştirgeci

TABLE OF CONTENTS

LIST OF FIGURES

Figure **Page**

LIST OF TABLES

Table **Page**

NOMENCLATURE

Alphabet

A_c	Minimum flow area	m^2
A_f	External fin surface area	m^2
A_o	Total surface area	m^2
A_i	Inner surface area of tube	m^2
A_p	Outer surface of tubes	m^2
A_{face}	Frontal face area	m^2
A_L	Crossectional area of tube occupied by liquid	m^2
A_{LD}	Dimensionless crossectional area of tube occupied by liquid	
A_V	Crossectional area of tube occupied by vapor	m^2
A_{VD}	Dimensionless crossectional area of tube occupied by vapor	m^2
C_i	Compressor coefficient	
C_{min}	Minimum heat capacity rate	j/Ks
C_{max}	Minimum heat capacity rate	j/Ks
C_r	Heat capacity ratio	
$C_{p,air}$	Specific heat for air	j/kgK
$C_{p,air,s}$	Saturation specific heat for air	j/kgK
$C_{p,air,m}$	Saturation specific heat for moist air	j/kgK
D_c	Fin collar outside diameter	m
D_h	Hydraulic diameter	m
d_o	Outside tube diameter	m
d_i	Inside tube diameter	m
f	Fanning friction factor	
f_V	Vapor refrigerant friction factor	
f_L	Liquid refrigerant friction factor	
Fr_{Liq}	Liquid Froude number	
F_l	Fin length	m

F_p	Fin pitch	m
F_s	Fin spacing	m
$f_{tp,stratifiedwavy,f}$	Stratified wavy region friction factor	
$f_{i,annular}$	Annular region friction factor	
$f_{i,annular*}$	Annular region friction factor correction auxiliary correlation for dry out region	
f_i	Interfacial roughness factor	
F_v	Volumetric efficiency correction factor	
g	Acceleration of gravity	m/s^2
G	Total mass velocity of liquid and vapor	kg/m^2s
G_{air}	Air mass flux based on the minimum free flow	
G_{strat}	Stratified flow transition mass velocity	kg/m^2s
G_{wavy}	Wavy flow transition mass velocity	kg/m^2s
$G_{wavy,xIA}$	Wavy flow transition mass velocity with x_{IA}	kg/m^2s
G_{mist}	Mist flow transition mass velocity	kg/m^2s
G_{bubbly}	Bubbly flow transition mass velocity	kg/m^2s
G_{dryout}	Dryout flow transition mass velocity	kg/m^2s
h_{ref}	Refrigerant side heat transfer coefficient	W/m^2K
h_{air}	Dry Air side heat transfer coefficient	W/m^2K
$h_{air,w}$	Wet Air side heat transfer coefficient	W/m^2K
h_c	Convective condensation heat transfer coefficient	W/m^2K
h_{cb}	Convective boiling heat transfer coefficient	W/m^2K
h_{dryout}	Dryout heat transfer coefficient	W/m^2K
h_{mist}	Mist flow heat transfer coefficient	W/m^2K
h_{nb}	Nucleate boiling heat transfer coefficient	W/m^2K
h_v	Vapor convective heat transfer coefficient	W/m^2K
h_{wet}	Heat transfer coefficient for the wet perimeter	W/m^2K
h_f	Nusselt film condensing coefficients on top perimeter of tube	

h_{tp}	Local perimeter averaged heat transfer coefficient	W/m^2K
h_{sp}	Single phase heat transfer coefficient	W/m^2K
h_{Ld}	Dimensionless vertical height of liquid	
h_{LV}	Latent heat of refrigerant vaporization	J/kg
h_{ref}	Refrigerant heat transfer coefficient	W/m^2K
H_{coil}	Coil height	m
k_{tube}	Conductive heat transfer coefficient for tube	W/mK
k_L	Thermal conductivity of liquid phase	W/mK
k_V	Thermal conductivity of vapor phase	W/mK
k_{ref}	Thermal conductivity refrigerant	W/mK
L_p	Louver Pitch	m
L_l	Louver length	m
L_h	Louver height	m
L_{coil}	Coil length	m
L_{seg}	Segment length	m
L_{coil}	Coil length	m
$\dot{m}$	Mass flow	kg/s
m	Intermediate parameter for fin efficiency calculation	
$m_{f,w}$	Intermediate parameter for fin efficiency calculation	
M	Molecular weight	g/mol
N	Number of lonitudinal tube rows	
N_t	Number of tubes	
N_f	Number of fin	
NTU	Number of transfer units	
NTU_a	Number of transfer units for air	
P_d	Wave height	m
P_t	Tube pitch	m
P_l	Row pitch	m

P	Pressure	Pa
P_{crit}	Critical pressure	Pa
P_r	Reduced pressure	Pa
P_{id}	Dimensionless perimeter of interface	
r_r	Radius ratio	
Pr_L	Prandtl number in liquid phase	
Pr_V	Prandtl number in vapor phase	
Pr_{ref}	Refrigerant Prandtl number	
Rh_{indoor}	Indoor air relative humidity	%
$Rh_{outdoor}$	Outdoor air relative humidity	%
q	Heat flux	W/m^2
q_{crit}	Critical heat flux	W/m^2
Re_{Dc}	Reynold number with collar diameter	
Re_{Din}	Reynold number with inner diameter	
Re_H	Homogenous Reynolds number	
Re_V	Reynolds number for vapor phase	
Re_δ	Reynolds number of liquid film	
S_s	Breadth of a slit in the direction of air flow	m
S_h	Height of slit	m
S_n	Number of slit per row	
S_w	Width of slit	m
X_l	Geometric parameters that correlated to P_t	m
X_m	Geometric parameters that correlated to P_l	m
X_f	Half wave length of fin wave	m
x	Vapor quality	
x_{de}	Dryout completion quality	
x_{di}	Dryout inception quality	
x_{IA}	Vapor quality at transition from intermittent	
X_{tt}	Lockhart- Martinelli parameter	
t_s	Evaporation temperature	^oC
t_d	Condensation temperature	^oC

$T_{a,in}$	Inlet air temperature	^oC
$T_{a,out}$	Outlet air temperature	^oC
$T_{c,s}$	Coil surface temperature	^oC
$T_{c,i}$	Cold side inlet temperature	^oC
$T_{c,in}$	Compressor inlet evaporation temp. after calculation	^oC
$T_{c,o}$	Cold side outlet temperature	^oC
$T_{comp,c}$	Compressor condensation temp. in iteration	^oC
$T_{comp,e}$	Compressor evaporation temp. in iteration	^oC
$T_{comp,sc}$	Compressor subcooling temp.	^oC
$T_{comp,sh}$	Compressor superheat temp.	^oC
$T_{cond,sc}$	Condenser outlet subcooling temp. value after calculation	^oC
$T_{h,i}$	Hot side inlet temperature	^oC
$T_{h,o}$	Hot side outlet temperature	^oC
T_{indoor}	Indoor air temperature	^oC
T_p	Tube pitch	m
T_d	Tube depth	m
T_{fin}	Fin thickness	m
$T_{outdoor}$	Indoor air temperature	^oC
$T_{suct,e}$	Suction copper tube outlet evaporation temp. value after calculation	^oC
$T_{suct,sh}$	Suction copper tube outlet superheat temp. value after calculation	^oC
u_L	Liquid refrigerant velocity	m/s
u_V	Vapor refrigerant velocity	m/s
u_{air}	Air velocity	m/s
W_{coil}	Coil width	m
We	Weber number	
We_V	Vapor Weber number	
We_L	Liquid Weber number	

$We_{L,xdi}$	Liquid weber number with x_{di}	
$(We/Fr)_L$	Liquid weber number and Froude number ratio	
Y	Correction factor	
Greek letter		
α	Void fraction	
δ	Liquid film thickness	m
Γ	Mass flow rate per unit width of the tube	kg/sm
ΔP_{disch}	Discharge line pressure drop	kpa
ΔP_{suct}	Suction line pressure drop	kpa
ΔP_f	Friction pressure term	Pa
ΔP_a	Acceleration pressure term	Pa
ΔP_g	Gravitational pressure term	Pa
$\Delta P_{f,L}$	Liquid frictional pressure drop	Pa
$\Delta P_{f,V}$:	Vapor frictional pressure drop	Pa
$\Delta P_{f,G}$:	Gravitational term	
$\Delta P_{annular,f}$	Frictional pressure drop in annular region	Pa
$\Delta P_{annular,f*}$	Frictional pressure drop in annular region with x_{di}	Pa
$\Delta P_{slug+intermittent,f}$	Frictional pressure drop in slug+intermittent region	Pa
$\Delta P_{stratifiedwavy,f}$	Frictional pressure drop in stratified wavy region	Pa
$\Delta P_{stratifiedwavy,1}$	Frictional pressure drop in stratified wavy region auxiliary corr.	Pa
$\Delta P_{dryout,f}$	Frictional pressure drop in dryout region	Pa
$\Delta P_{sp,f,m,xde}$	Single phase frictioanal pressure drop with	Pa
$\Delta P_{mist,f*}$	Frictional pressure drop in stratified wavy region auxiliary correlation for dryout region calculations	Pa
$\Delta P_{mist,f}$	Frictional pressure drop in mist region auxiliary correlation	Pa

ε	Effectiveness	
ε_h	Intermediary term for vapor void fraction calculation	
ε_{ra}	Intermediary term for vapor void fraction calculation	
ε_{VV}	Vapor void fraction	
$\varepsilon_{VV,xIA}$	Vapor void fraction with x_{IA}	
ε_a	Effectiveness for air	
ε_{sp}	Single phase effectiveness	
ε_{tp}	Two phase effectiveness	
η_{surf}	Dry surface efficiency	
$\eta_{surf,w}$	Wet surface efficiency	
η_f	Dry fin efficiency	
$\eta_{f,w}$	Wet fin efficiency	
Θ	Corrugation angle	rad
Θ_l	Louver angle	rad
Θ_{strat}	Stratified flow angle of tube perimeter	rad
Θ_{dry}	Dry angle of tube perimeter	rad
μ	Dynamic viscosity	Ns/m^2
μ_L	Liquid refrigerant dynamic viscosity	Ns/m^2
μ_V	Vapor refrigerant dynamic viscosity	Ns/m^2
μ_f	Dynamic viscosity of water	Ns/m^2
μ_{ref}	Dynamic viscosity of refrigerant	Ns/m^2
μ_m	Refrigerant homogenous dynamic viscosity	Ns/m^2
$\mu_{m,xde}$	Refrigerant homogenous viscosity with x_{de}	Ns/m^2
ν	Specific volume	m^3/kg
ξ	Factor	
ρ_V	Vapor density	
ρ_L	Liquid density	kg/m^3
$\rho_{,ref,in}$	Refrigerant inlet density	kg/m^3
$\rho_{,ref,out}$	Refrigerant outlet density	kg/m^3

$\rho_{,ref}$	Refrigerant density	kg/m^3
ρ_m	Refrigerant homogenous density	kg/m^3
σ	Surface tension	N/m
Ø	Intermediate parameter for fin efficiency calculation	
$Ø_{liq}$	Two phase correction factor	

CHAPTER 1

INTRODUCTION

Air conditioning/refrigeration with vapor-compression cycle was commercialized in 1911. This commercializing was enabled advancement in distinct fields from air conditioning to transportation of foods. Therefore, cooling with vapor compression cycle became a necessity for everyone. Here we focus on the vapor compression cycle specifically used for space cooling applications such as household and office air conditioning, cold room units and data center cooling. These systems are the most common ones.

Generally, two working fluids (air and water) are being used in air conditioning applications. The energy of the working fluid is transferred to the coolant at the evaporator. Then it is discharged to the ambient at the condenser. Here, we benefit from the current heat exchanger designs and their heat transfer calculations in the literature and also from the compressor correlations in order to investigate how the compressor cycle can be simulated in various air conditioning applications.

There are many distinct evaporator and condenser designs both on the market and in the literature; however, heat pump vapor compression cycle simulation software is very rare, i.e. only 3: EvapCond [1], ACHP [2], RooftopSelector [3]. The market and literature require a simulation program which simulates the effect of all the components in the refrigeration cycle instantly due to several reasons. First, designers generally use a specific program for heat exchanger design and another for selecting compressor. In order to assure the most appropriate equipment selection, iterative calculation method is essential. In addition, the current approach pressure equalization is overlooked as a result of which causes a lot of problems on the field.

1.1 AIR CONDITIONING DESIGN METHODOLOGY

A typical air conditioner system has four main components: compressor, condenser,

expansion valve and evaporator. Another essential component in the vapor compression cycle is the type of the refrigerant, because it changes the entire characteristics of the cycle. Therefore, it is a never-ending process for new refrigerants to be developed for many distinct applications. Currently developed refrigerants have relatively decreased effects on the environment in comparison to their predecessors. Until very recently R410a and R134a refrigerants were common, but nowadays R32 and R1234yf refrigerants are being used on the market. Furthermore, with the new regulations such as ERP 2018 and ERP 2021, the expected seasonal efficiency values are being increased for the commercial units.

Due to the expectations of the market and regulations, the effect of the refrigerants on the environment is going to be decreasing. Nowadays, refrigerants are released to the market according to their GWP (Global warming potential). Old and new refrigerant GWP and Ozone Depletion Potential (ODP) values are listed in the Table1.1.

Table 1-1 Refreigerant's GWP and ODP (Source:[4])

	Refrigerant	OWP	GWP
Old	R22	0,055	1810
Old	R410A	0	2088
Old	R134A	0	1430
New	R32	0	675
New	R1324yf	0	4

In addition to the developments related with the refrigerants, the developments on the other equipment are also being continued. For instance; frequency inverter compressors are taking place of on/off compressors, microchannel heat exchangers are preferred to finned tube heat exchangers. However, due to the microchannel evaporator refrigerant distribution problems, it is generally used as condenser in heat pump systems.

Finned tube heat exchanger simulation models have been developed since 1980s, and many researchers have studied the mathematical model of simulations and empirical heat transfer equations. While tube by tube and segment by segment methods have been developed for circuit arrangement [5] [6] [7], refrigerant and air side heat transfer coefficient correlation studies also have been done according to these methods. Furthermore, Domanski et al. managed to programme ISHED which can learn circuit analyze logic. [8]

1.2 HEAT EXCHANGER TYPES IN COMPRESSOR CYCLE

On the market, compressor cycle commercial units appear in two categories; air and water cooled. As well as the air finned tube and microchannel heat exchangers, the water plate and shell & tube heat exchangers are used for cooling and heating.

1.2.1 Finned Tube Heat Exchanger

Finned tube heat exchangers are being used for heating and cooling the air on the market. They are not only being used in compressor cycle, but also can condition the air with steam and water. Table 1.2 lists in which applications finned tubes can be used.

Table 1-2 Heat exchanger and flow types

Type	Primary flow	Secondry flow
Evaporator	Air/water	Refrigerant
Condenser	Air/water	Refrigerant
Water cylce heat exc.	Air/water	Water
Steam cycle heat exc.	Air/water	Steam

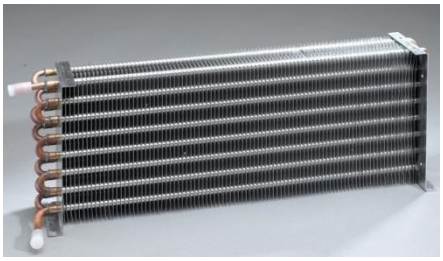

Figure 1-1 Visual of finned tube heat exchanger (Source: [9])

On finned tube heat exchangers, various fin types such as wavy, plain, louver, slit, are used for increasing the heat transfer between air and the refrigerant. Also grooved or smooth type copper tubes are used for the refrigerant side.

1.2.2 Microchannel heat exchangers

The applications in which microchannel heat exchangers are used similar to finned tube heat exchangers, i.e. heating/cooling applications. Although these type of heat exchangers are small (small volume for the same or greater heat transfer surface area) and need less refrigerants for the same capacity range compared to finned tube heat exchangers, they are not preferred due to non-uniform refrigerant distribution problem.

Figure 1-2 Microchannel heat exchanger (Source: [10])

1.2.3 Shell & tube heat exchangers

Shell & tube heat exchangers are being used in many distinct applications. For specifically cooling applications, they are preferred for conditioning the water in the compressor cycle. Shell & tube designs are usually used with 5^{o}C water temperature difference to assure desired heat transfer. While they require more refrigerant than other heat exchangers, they are preferred due to their high capacity.

1.2.4 Plate heat exchangers

The applications in which plate heat exchangers are preferred are the same with the Shell & tube heat exchangers. There are gasket and brazed type heat exchangers. Gasket plate heat exchangers can be repaired on blockage problems, and its surface area can be increased because they can be disintegrated and montaged with changes. However, brazed types cannot

be disintegrated (brazing connects all the parts similar to they are welded), therefore, brazed types should be replaced when repair is required.

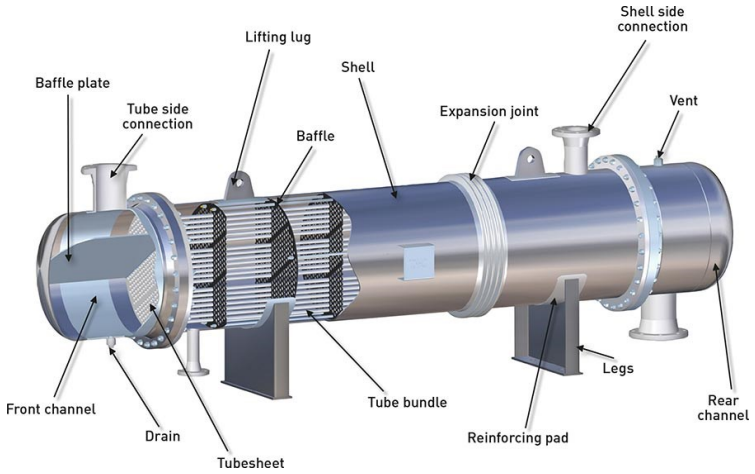

Figure 1-3 Shell & tube heat exchanger (Source: [11])

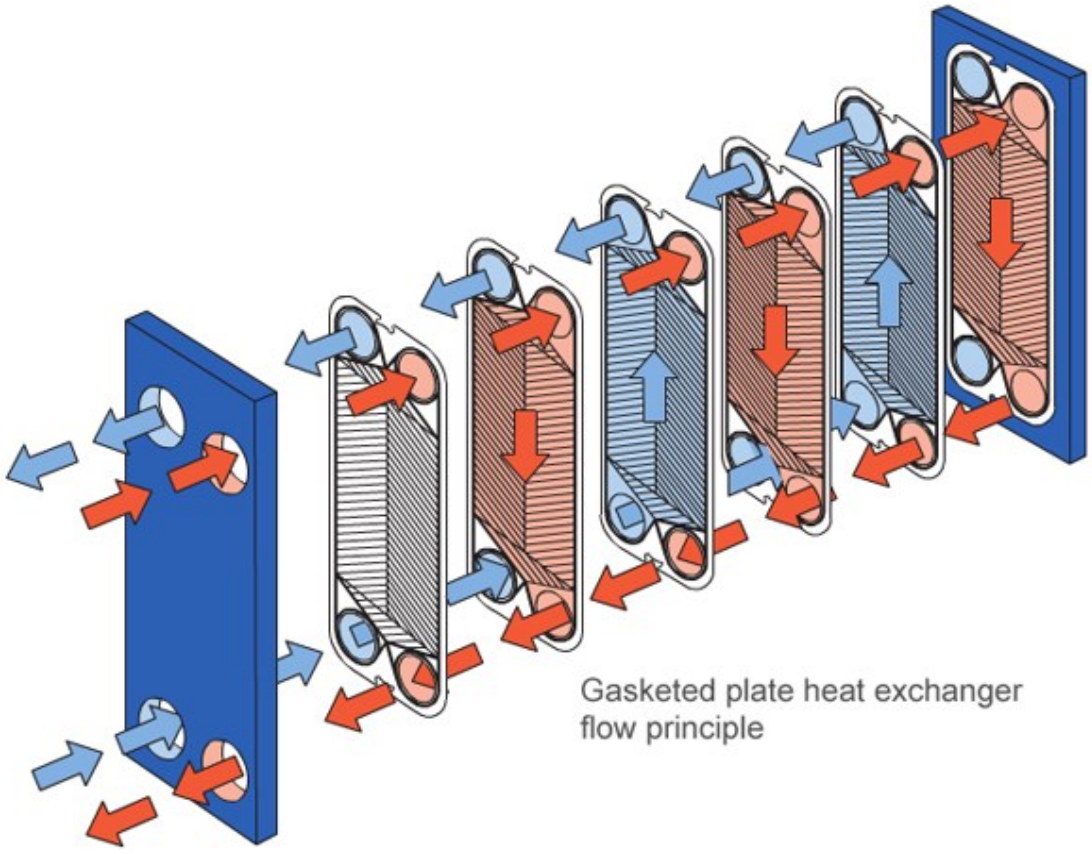

Figure 1-4 Gasket plate exchangers (Source: [12])

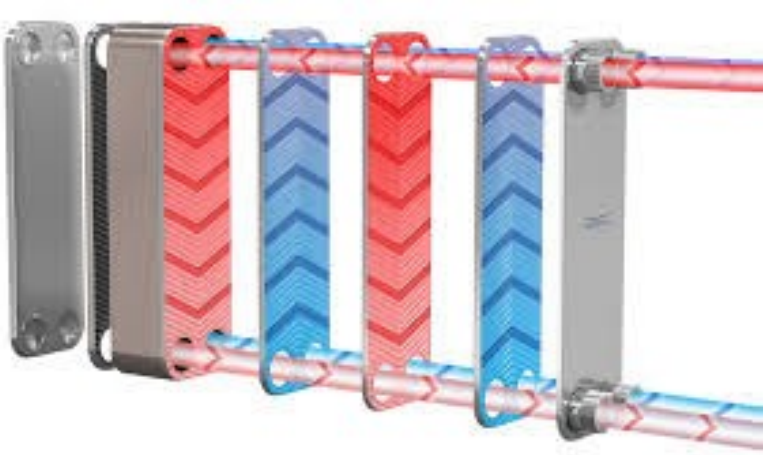

Figure 1-5 Plate heat exchangers (Source: [13])

1.3 COMPRESSOR TYPES

There are three main types of compressors which are, piston, scroll and screw. Although scroll and screw types are taking place of piston compressor. The fact that piston compressors are repairable makes them preferable in the market. The most important difference between screw and scroll types is their capacity range. While scroll compressors are up to 100 kw capacity range screw compressor can reach 500kw cooling capacity [14] [15]. Furthermore, because frequency inverter adaption can be applied to this type of compressors, they provide advantages of energy efficiency and power consumption for the consumers.

Figure 1-6 1-Semi hermetic piston compressor (Source: [16]) 2-Scroll compressor (Source: [17]) 3-Screw compressor (Source: [18])

1.4 OTHER EQUIPMENT

Compressor cycle also consists some auxiliary equipment that help the system work properly such as filter dryer, liquid receiver, suction accumulator, ball valve etc. Auxiliary equipment calculations are not examined in this study. Their brief explanation can be found below.

Filter dryer: Filter dryer is used for filtering and dehumidifying the refrigerant in the cycle. Bi-flow and non-return types are on the market.

Liquid receiver: Liquid receiver is used for balancing the refrigerant mass in the system, that the condenser and evaporator are not compact in a unit.

Suction accumulator: This equipment is used for protecting the unit by eliminating return of liquid to compressor.

Ball valve: Ball valve is used for closing the liquid line while fixing the units.

Figure 1-7 Filter dryer (Source: [19])

Figure 1-8 Liquid receiver (Source: [20])

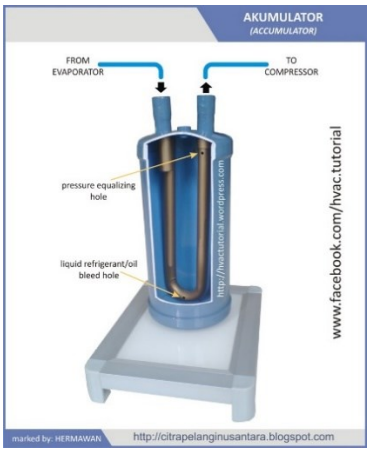

Figure 1-9 Suction accumulator (Source: [21]), Ball valve (Source: [22])

CHAPTER 2

COMPONENT MODEL DEVELOPMENT

There are four major components in a typical HVAC system: compressor, condenser, expansion device and evaporator. Compressor compresses the superheated refrigerant from low pressure to high pressure via rotary or reciprocating motion supplied from work input. The refrigerant in the evaporator evaporates while receiving heat from its surrounding. Therefore, evaporators are used for cooling applications. Similarly, phase change occurs in condensers, and therefore heat is transferred from the refrigerant to the environment in condensers. Furthermore, expansion devices are used to decrease the pressure of sub-cooled high pressure refrigerant to low pressure while the expansion process occur at constant enthalpy.

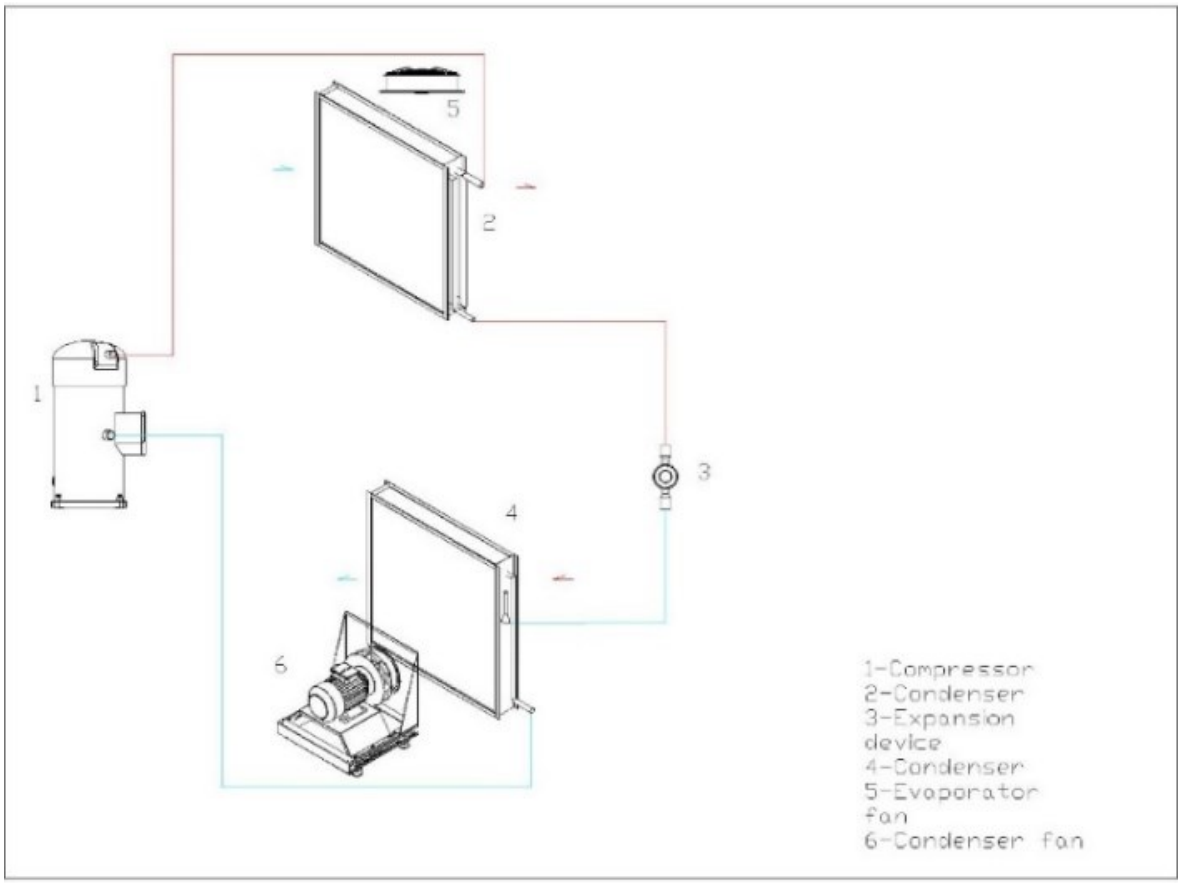

Figure 2-1 Compressor cycle schematic

2.5 Calculation Methods of Compressor Cycle Main Equipment

2.5.1 Compressor calculations

In HVAC, scroll and reciprocating compressor types are commonly used. Most common performance calculation is rating standart of ARI model [23], which includes the polynomial coefficients of suction and discharge saturation temperatures of compressors. Each coefficient in formula is valid for the specific rating conditions. So, compressor manufacturers are publishing Ci and Di coefficients to calculate the refrigeration capacity, power input, mass flow and current of a specific compressor.

$$X = C1 + C2\,t_s + C3\,t_d + C4\,t_s^2 + C5\,t_s t_d + C6\,t_d^2 + C7\,t_s^3 + C8\,t_d t_s^2 + C9\,t_s t_d^2 + C10 t_d^3 \quad (2.1)$$

To be able to calculate the change of capacitive values according to the other superheat values, mass flow should be corrected. [23]. A change of the superheat temperature has a negligible impact on power consumption.

$$\dot{m}_{corrected} = \{1 + Fv\,[(v_{rated}/v_{corrected}) - 1]\} \cdot \dot{m}_{rated} \quad (2.2)$$

Besides, subcooling degree can be changed in practical area. So, compressor capacity and COP values should be corrected according to the enthalpy difference.

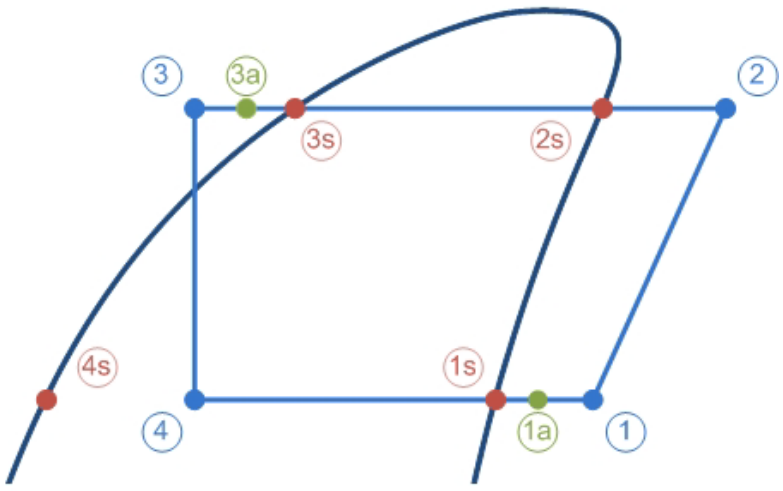

Figure 2-2 Compressor cycle in PH diagram

$$Q_{comp,corr} = \dot{m}_{corrected}(h_3 - h_{3s}) \tag{2.3}$$

$$COP_{corr} = \frac{Q_{comp,corr}}{Q_{p,in}} \tag{2.4}$$

2.5.2 Finned tube heat exchanger calculations

2.5.2.1 Method

Finned tube heat exchanger calculations are differed on three basic calculation method respectively, zone-by-zone, tube-by-tube and segment-by-segment. These methods have advantages to each other. While, tube-by-tube and segment-by-segment models are detailed to analyze heat exchanger circuit design, and proper to use of row-by-row air side heat transfer coefficients, zone-by-zone method does not have these capabilities, however more computationally efficient. In figure 2-3 discretization methods are shown.

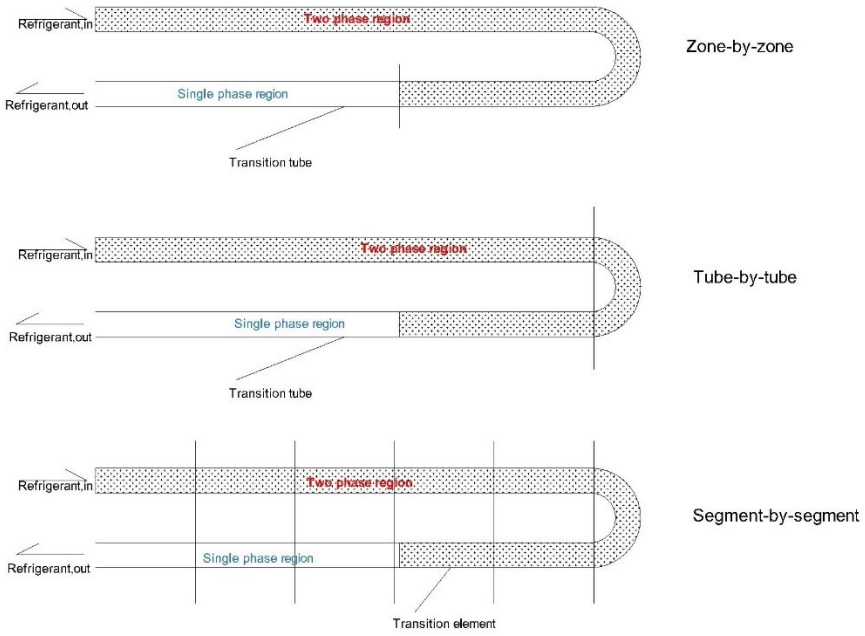

Figure 2-3 Heat exchanger calculation models

2.5.2.1.1 Zone-by-zone method

Zone by zone calculation method is based on refrigerant position. While, in condenser, there are three zones, named superheated, two phase and subcooled; in evaporator, there are two zones, named two phase and superheated [24]. This calculation method assumes every circuit is the same. Because of that different circuit designs cannot be applied simultaneously.

2.5.2.1.2 Tube-by-tube method

Tube-by-tube method assumes that, each single tube is a calculation domain [7]. Because of that, this method allows circuitry algorithm. Inlet and outlet refrigerant properties are constant along the tube. Although this approach requires long computational time, it gives more accurate results than zone-by-zone method. Furthermore, the transition tube can give calculation error because of the constant properties of the refrigerant.

2.5.2.1.3 Segment-by-segment method

Segment-by-segment method defines segments in each tube [25]. With this method, transient tube calculation error problem is passed. But, as the segment number increases, computational time increases greatly. Refrigerant properties change after every single segment. Segment by segment calculations can also be adapted to the tube-by-tube calculations by making the segment number 1. Elemental method captures not only the circuitry effect, but also air maldistribution.

2.5.2.2 Heat transfer methods

2.5.2.2.1 **ε-NTU** Method

For the calculation of heat exchanger performance, if the inlet temperatures are known, it is preferable to use the effectiveness-number of transfer units (ε-NTU) method,

which simplifies the algebra involved in predicting the performance of complex flow arrangements. Although ε-NTU Method is the most proper method for the elemental models, because the transition element can be occurred, iteration can give incorrect results. In ε-NTU method, single and two-phase regions should be applied [26].

Dry conditions

$$Q = \varepsilon C_{min}\left(T_{h,in} - T_{c,in}\right) \tag{2.5}$$

$$NTU = UA/C_{min} \tag{2.6}$$

Effectiveness can be calculated as follows

For single phase:

If C_{min} is unmixed and C_{max} is mixed,

$$\varepsilon_{sp} = \frac{1}{C_r}\left(1 - exp\{-C_r[1 - exp(-NTU)]\}\right) \tag{2.7}$$

If C_{min} is mixed and C_{max} is unmixed,

$$\varepsilon_{sp} = 1 - exp\left\{-\frac{1}{C_r}[1 - exp(-C_r NTU)]\right\} \tag{2.8}$$

If both C_{min} and C_{max} are unmixed, [27]

$$\varepsilon_{sp} = 1 - exp\left\{-\frac{1}{C_r} NTU^{0.22}[exp(-C_r NTU^{0.78})]\right\} \tag{2.9}$$

The unmixed or mixed state of the fluid is determined by the geometry of the fluid flow passages. Flow through a louvered fin heat exchanger is considered mixed since the perforated surface of the louvered fin accommodates cross.mixing of the flow paths. Flow through nonperforated fin heat exchangers is considered unmixed since there is no mechanism for mixing. On the refrigerant side, the refrigerant is always considered unmixed in the

segment-by-segment calculation. The unmixed C_{min} and C_{max} equation is more suitable for heat exchangers with smooth fins. Correlations for dry conditions are below. [27]

For two-phase:

$$\varepsilon_{tp} = 1 - exp\ (-NTU) \tag{2.10}$$

Where

$$C_r = C_{min}/C_{max} \tag{2.11}$$

Where C_{min} is the minimum value of air and refrigerant heat capacitance, C_{max} is the maximum value of air and refrigerant heat capacitance.

$$C_{air} = \dot{m}_{air} c_{p,air} \tag{2.12}$$

$$C_{ref} = \dot{m}_{ref} c_{p,ref} \tag{2.13}$$

Wet conditions

Wet conditions affect heat exchanger effectiveness and heat capacitance ratio calculations. In addition, air side specific heat value is taken at saturation temperature and number of transfer unit calculation logic is the same as the dry surface calculations [5].

$$Q = \varepsilon_{wet} \dot{m}_{air} \left(h_{air,in} - h_{ref,in,sat}\right) \tag{2.14}$$

For single phase:

$$\dot{m}_{ref} cp_{ref} > \dot{m}_{air} cp_{air}$$

$$\varepsilon_{wet} = \frac{1}{C_{r,w}} \left(1 - exp\{-C_{r,w}[1 - exp(-NTU_w)]\}\right) \tag{2.15}$$

$$\dot{m}_{ref} cp_{ref} < \dot{m}_{air} cp_{air}$$

$$\varepsilon_{wet} = 1 - exp\left\{-\frac{1}{C_{r,w}}\left[1 - exp\left(-C_{r,w} NTU_w\right)\right]\right\} \tag{2.16}$$

Where Cr,w is min value of these both

$$\frac{\dot{m}_{ref} c_{p,ref}}{\dot{m}_{air} c_{p,sat}}, \frac{\dot{m}_{air} c_{p,sat}}{\dot{m}_{ref} c_{p,ref}}$$

Two phase flow:

$$\varepsilon_w = 1 - exp(-NTU_w) \tag{2.17}$$

$$NTU_w = \frac{UA_w}{m_{air}} \tag{2.18}$$

2.5.2.2.2 LMTD Method

Log Mean Temperature Difference method is another option to calculate the heat transfer rate. In this method, outlet temperature is needed in order to perform calculations. Hence, if inlet temperatures are known, LMTD method requires iterative procedures. Heat exchanger capacity by using LMTD method can be calculated as follows [26]:

For parallel flow:

$$Q = UA(LMTD) \tag{2.19}$$

$$LMTD = \frac{\Delta T_2 - \Delta T_1}{\ln\left(\Delta T_2 - \Delta T_1\right)} \tag{2.20}$$

$$\Delta T_1 = T_{h,i} - T_{c,i} \tag{2.21}$$

$$\Delta T_2 = T_{h,o} - T_{c,o} \tag{2.22}$$

For counter flow:

For counter flow heat exchangers, the correction factor (F) is unity.

$$Q = UA(LMTD) \tag{2.23}$$

$$LMTD = \frac{\Delta T_2 - \Delta T_1}{\ln(\Delta T_2 - \Delta T_1)} \tag{2.24}$$

$$\Delta T_1 = T_{h,i} - T_{c,o} \tag{2.25}$$

$$\Delta T_2 = T_{h,o} - T_{c,i} \tag{2.26}$$

2.5.2.3 Heat transfer equations

In order to calculate overall heat transfer rate of the heat exchanger, thermal circuit model should be considered. In steady state, heat is transferred from the hot fluid to the cold fluid through the wall. During conduction, via tube and fin, the subsequent deposition of a film on the surface can greatly increase the resistance to heat transfer between fluids. Therefore, fouling factor should be considered and inserted to the thermal resistance. While dry condition calculations are as in the traditional heat transfer method, [28] wet surface conditions shown below are modified by Harms et al. [5]

$$\frac{1}{UA} = \frac{1}{U_c A_c} = \frac{1}{U_h A_h} \tag{2.27}$$

$$\frac{1}{UA} = \frac{1}{(\eta_o hA)_c} + \frac{R_{f,c}''}{(\eta_o A)_c} + R_w + \frac{R_{f,h}''}{(\eta_o A)_h} + \frac{1}{(\eta_o hA)_h} \tag{2.28}$$

If the fouling terms for fin and tube heat exchangers are neglected,

Dry conditions:

$$\frac{1}{UA} = \frac{1}{h_{ref} * A_{in}} + ln\left(\frac{(\frac{D_o}{D_i})}{2\pi k_{tube} L_{tube}}\right) + \frac{1}{(\eta_{surf} h_{air} A_o)} \tag{2.29}$$

Wet conditions:

$$\frac{1}{UA_w} = \frac{c_{p,air,s}}{h_{ref} A_{in}} + c_{p,air,s} ln\left(\frac{\frac{D_o}{D_i}}{2\pi k_{tube} L_{tube}}\right) + \frac{c_{p,air,m}}{\eta_{surf,w} h_{air} A_o} \tag{2.30}$$

Saturation specific heat is calculated as a derivative of saturated air enthalpy at refrigerant temperature:

$$c_{p,air,s} = \frac{dh_{air,s}}{dT} \tag{2.31}$$

Where surface and fin efficiencies are calculated according to wet and dry conditions. If the coil surface temperature is below the air saturation temperature, dry and wet surface fin efficiencies are shown below according to the Harms et al. method [5].

$$\eta_{surf} = 1 - \frac{A_f}{A_o}(1 - \eta_f) \tag{2.32}$$

$$\eta_{surf,w} = 1 - \frac{A_f}{A_o}(1 - \eta_{f,w}) \tag{2.33}$$

Where fin efficiency;

For dry conditions

$$\eta_f = \frac{tanh\ (mD_{collar}\emptyset)}{m * D_{collar}\emptyset} \tag{2.34}$$

$$m = \sqrt{(\frac{2h_{air}}{2k_{fin}t_{fin}})} \tag{2.35}$$

For wet conditions

$$\eta_{f,w} = \frac{tanh\left(m_{f,w} D_{collar} \emptyset\right)}{m_{f,w} D_{collar} \emptyset} \tag{2.36}$$

$$m_{f,w} = \sqrt{\left[\frac{2\left(F_p + t_{fin}\right) h_{air,w} c_{p,air,s}}{k_f F_p t_{fin} c_{p,air}}\right]} \tag{2.37}$$

$$d_{collar} = d_o + 2t_{fin} \tag{2.38}$$

$$\emptyset = (r_r - 1)[1 + 0{,}35ln\ (r_r)] \tag{2.39}$$

Radius ratio is defined for staggered tubes:

$$r_r = 1{,}27 \frac{X_m}{d_{collar}} \sqrt{[\frac{X_l}{X_m} - 0{,}3]} \tag{2.40}$$

Where X_l and X_m are geometric parameters that are correlated to the tube pitch (P_t) and row pitch (P_l) as follows:

$$X_m = \frac{P_t}{2}\ if\ P_t \leq P_l \tag{2.41}$$

$$X_m = P_l\ if\ X_m > P_l \tag{2.42}$$

$$X_l = \frac{1}{2} \sqrt{(\frac{P_t}{2})^2 + {P_l}^2} \tag{2.43}$$

Where colar radius is the tube outside radius including fin collar.

In order to decrease calculation time, Braun et all [5] recommends the calculation method mentioned below to find out the air outlet temperature and enthalpy according to wet and dry conditions.

Outlet air conditions for dry conditions

$$T_{a,out} = T_{a,in} + \varepsilon_a (T_{c,s} - T_{a,in}) \tag{2.44}$$

$$NTU_a = \frac{\eta_{surf} h_{air} A_o}{C_{p,air}} \tag{2.45}$$

$$\varepsilon_a = 1 - e^{-NTU_a} \tag{2.46}$$

Outlet air conditions for wet conditions, b33

$$T_{a,out} = T_{a,in} + \varepsilon_a (T_e - T_{a,in}) \tag{2.47}$$

$$h_{a,out} = h_{a,in} + \varepsilon_a (h_{s,c} - h_{a,in}) \tag{2.48}$$

$$NTU_a = \frac{\eta_{surf,w} h_{air,w} A_o}{C_{p,air}} \tag{2.49}$$

$$\varepsilon_a = 1 - e^{-NTU_a} \tag{2.50}$$

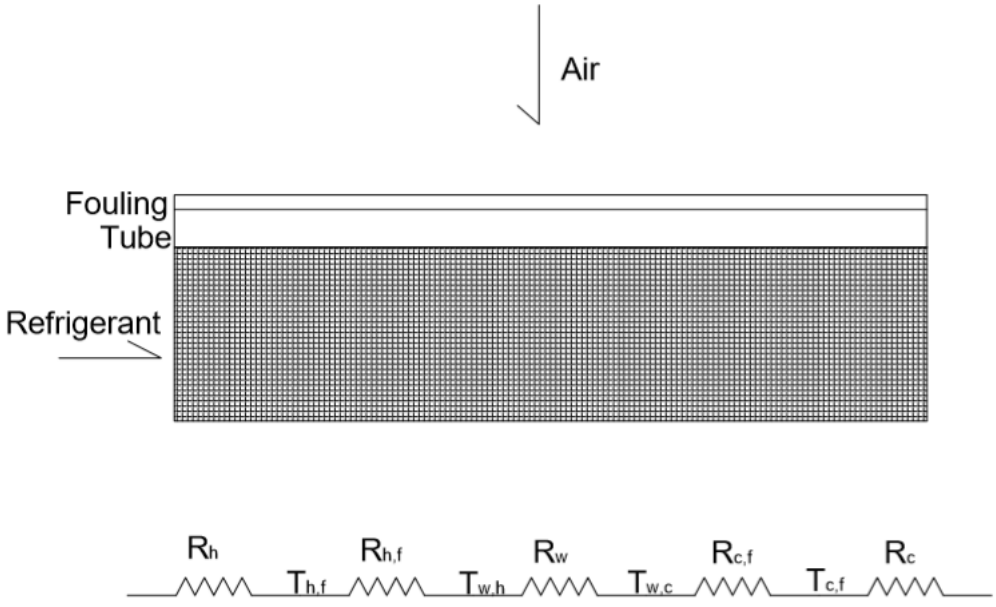

Figure 2-4 Heat transfer ratio electrical analogy

2.5.2.4 Junction tube matrix

To simulate air outlet conditions and refrigerant outlet conditions junction tube matrix is being used with segment by segment method. With this method two-dimensional non-uniformity of air distribution can be applied. A change in the single and two-phase segment can be obtained according to segment number arrangement, as well. Moreover, different circuitry algorithms can be applied with this method and most effective heat exchanger capacity solution can be found.

The term 'junction' is defined as the intersection where two or more tubes are joined together [25].The relationships are shown as follows:

JTA[n,i,j]=1 :junction n is upstream and connected to tube at row i column j

JTA[n,i,j]=-1 :junction n is downstream and connected to tube at row i column j

JTA[n,i,j]=0 :junction n is not connected to tube at row i column j

According to the information in the junction tube connectivity matrix, the following can be determined:

- Refrigerant phase position and pressure drops can be calculated
- Refrigerant mass flow in each circuit can be calculated
- Different working fluids in different circuits can be calculated

In the study of Jiang et al. a sample circuit schema, table and model assumptions are shown below [25]. Each segment is treated as a discrete unit of heat transfer, without considering the conduction of heat transfer through the fin plates between tubes.

When the air flow at the face of the heat exchanger is non-uniform (i.e. different air velocities at different segments of the tubes in the frontal face row), the air velocity at the segments in the air flow direction across the heat exchanger remains the same as that at the corresponding segment in the frontal face. The air side heat transfer coefficient for each segment is calculated based on the individual air velocity at that segment. When dehumidification occurs, the heat transfer resistance due to the water film on the surface of the tube and the fin, is either neglected or can be accounted for by adding a certain value of resistance to the fin-tube contact resistance.

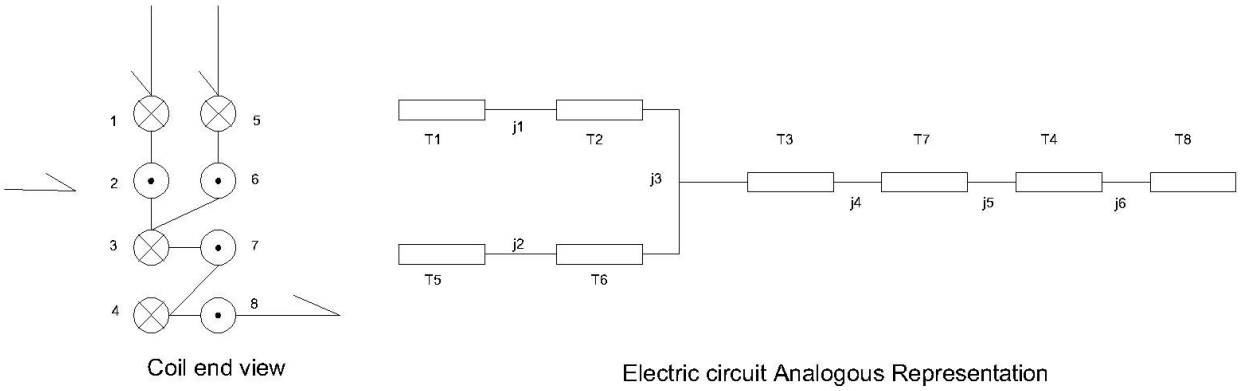

Figure 2-5 Circuit schematic (Source: [25])

Refrigerant pressure drop is calculated in each segment, and in each segment refrigerant properties are constant.

$$P_{i,j,k,in} - P_{i,j,k,out} = \Delta P_f + \Delta P_a + \Delta P_g \tag{2.51}$$

Where;

i: row number

j: column number

k: segment number for refrigerant flow

ΔP_f: Friction term

ΔP_a: Acceleration term

ΔP_g: Gravitational term

Pressure drop calculation will be detailed in section 2.1.2.6.

For staggered tube arrangement:

$$\dot{m}_{air,i,j+1,k,in} = 0{,}5\left(\dot{m}_{air,i,j,k,out} + \dot{m}_{air,i+1,j,k,out}\right) \tag{2.52}$$

$$\dot{m}_{air,i,j+1,k,in} h_{air,i,j+1,k,in} = 0{,}5\left(\dot{m}_{air,i,j,k,out} h_{air,i,out} + \dot{m}_{air,i+1,j,k,out} h_{air,i+1,j,out}\right) \tag{2.53}$$

$$\dot{m}_{air,i,j+1,k,in} * w_{air,i,j+1,k,in} = 0{,}5\left(\dot{m}_{air,i,j,k,out} w_{air,i,out} + \dot{m}_{air,i+1,j,k,out} w_{air,i+1,j,out}\right) \tag{2.54}$$

Table 2-1 Junction tube matrix index (Source: [25])

		Tube (row, column)							
		1,1	1,2	1,3	1,4	2,1	2,2	2,3	2,4
Junction	1	-1	1						
	2					-1	1		
	3		-1	1			-1		
	4			-1				1	
	5				1			-1	
	6				-1				1

For inline tube arrangement:

$$\dot{m}_{air,i,j+1,k,in} = \dot{m}_{air,i,j,k,out} \tag{2.55}$$

$$h_{air,i,j+1,k,in} = h_{air,i,j,k,out} \tag{2.56}$$

$$w_{air,i,j+1,k,in} = w_{air,i,j,k,out} \tag{2.57}$$

2.5.2.5 Air side heat transfer and pressure drop correlations

Air side and pressure drop correleations in the litterature are usually according to Colburn j and friction factor. Researchers have made a lot different tests and data reduction methods according to heat exchanger geometries. Although there are studies for wet surface conditions, most common cases are at the dry conditions.

$$j = \frac{h_{air}}{G_{air,max} c_{p,air}} {Pr_{air}}^{2/3} \tag{2.58}$$

$$f = \frac{A_c}{A_o}\frac{\rho_m}{\rho_1}\left[\frac{2\Delta P \rho_1}{{G_c}^2} - (1+\sigma^2)\left(\frac{\rho_1}{\rho_2} - 1\right)\right] \tag{2.59}$$

Correlations for plain, wave, louver and slit fins at dry surface conditions are shown below.

2.5.2.5.1 Plain fins:

For dry conditions; [29]

For N=1;

$$j = 0.108{Re_{Dc}}^{-0.29}(\frac{P_t}{P_l})^{j_1}(\frac{F_p}{D_C})^{-1.084}(\frac{F_p}{D_h})^{-0.786}(\frac{F_p}{P_t})^{j_2} \tag{2.60}$$

Where

$$j_1 = 1.9 - 0.23\ln{(Re_{Dc})} \tag{2.61}$$

$$j_2 = -0.236 + 0.126\ln{(Re_{Dc})} \tag{2.62}$$

For N≥2;

$$j = 0.086 * {Re_{Dc}}^{j_3}N^{j_4}(\frac{F_p}{D_C})^{j_5}(\frac{F_p}{D_h})^{j_6}(\frac{F_p}{P_t})^{-0.93} \tag{2.63}$$

Where

$$j_3 = -0.361 - \frac{0.42N}{ln(Re_{dc})} + 0.158\ln{(N(\frac{F_p}{D_c})^{0.41})} \tag{2.64}$$

$$\mathrm{j_4} = -1.224 - \frac{0.076(\frac{\mathrm{P_l}}{\mathrm{D_h}})^{1.42}}{\ln{(\mathrm{Re_{Dc}})}} \tag{2.65}$$

$$\mathrm{j_5} = -0.083 + \frac{0.058\mathrm{N}}{\ln{(\mathrm{Re_{Dc}})}} \tag{2.66}$$

$$\mathrm{j_6} = -5.735 + 1.21\ln{(\frac{\mathrm{Re_{Dc}}}{\mathrm{N}})} \tag{2.67}$$

$$\mathrm{f} = 0.0267{\mathrm{Re_{Dc}}}^{\mathrm{F1}}(\frac{\mathrm{P_t}}{\mathrm{P_l}})^{\mathrm{F2}}(\frac{\mathrm{F_p}}{\mathrm{D_c}})^{\mathrm{F3}} \tag{2.68}$$

$$\mathrm{F_1} = -0.764 + 0.739\frac{\mathrm{P_t}}{\mathrm{P_l}} + 0.177\frac{\mathrm{F_p}}{\mathrm{D_c}} - \frac{0.00758}{\mathrm{N}} \tag{2.69}$$

$$F_2 = -15.689 + \frac{64.021}{\ln(Re_{Dc})} \tag{2.70}$$

$$F_3 = -1.696 + \frac{15.695}{\ln(Re_{Dc})} \tag{2.71}$$

$$D_h = \frac{4A_c L}{A_0} \tag{2.72}$$

$$Re_{Dc} = \frac{G_{air,max} D_c}{\mu_{air}} \tag{2.73}$$

For wet conditions; [30]

300<ReDc<5500

$$j = 0.29773 Re_{Dc}^{-0.364} \varepsilon^{-0.168} \tag{2.74}$$

$$j = 0.4 Re_{Dc}^{-0.468+0.04076N} \varepsilon^{0.159} N^{-1.261} \tag{2.75}$$

$$f = 28.209 Re_{Dc}^{-0.5653} N^{-0.1026} \left(\frac{F_p}{D_c}\right)^{-1.3405} \varepsilon^{-1.3343} \tag{2.76}$$

$$\varepsilon = \frac{A_o}{A_p} \tag{2.77}$$

In 2007 Pirompugd et al. [31] used finite circular fin method for wet surfaces. In this method, heat exchangers divided into little segments and separated into three main region named respectively, fully dry, fully wet and partially wet. Although Wang and Pirompugd developed their correlations for plain and wave finned heat exchangers, correlations are still for narrow geometry ranges.

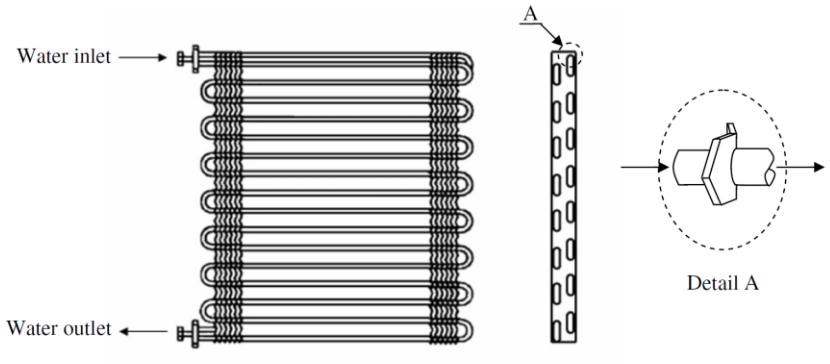

(a) Dividing the wavy fin-and-tube heat exchangers into may tiny segments

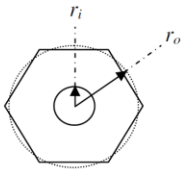

(b) Equivalent circular area method

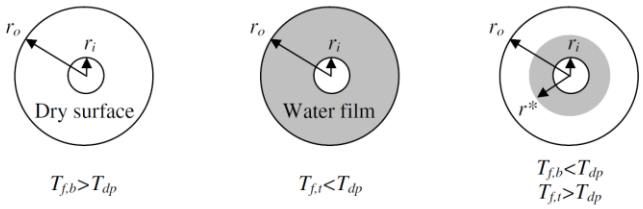

(c.1) Fully dry condition (c.2) Fully wet condition (c.3) Partially wet condition

(c) Circular fin in fully dry, fully wet and partially wet conditions

Fig. 3. Finite circular fin method (FCFM).

Figure 2.6 Air side fully dry, fully wet and partially wet conditions on the tubes (Source: [32])

For plain fins Pirompugd and Wang [33] published the correlations as added below.
Fully wet conditions: 1, 2, 4, 6 Rows and partially wet conditions 1, 2, 4 Rows

$$j = aRe_{Dc}^{\left(b\frac{F_s}{F_p}+c\frac{P_l}{D_c}+d\frac{P_t}{D_c}+e\right)} \tag{2.78}$$

$$j_{h,6,partial} = \left(738.92534\frac{F_s{}^2}{F_p{}^2} - 1390.12647\frac{F_s}{F_p} + 654.15084\right) Re_{Dc}^{\left(-230.74625\frac{F_s{}^2}{F_p{}^2}+434.90018\frac{F_s}{F_p}+205.41037\right)} \tag{2.79}$$

$$j_{m,6,partial} = \left(9483.51598\frac{{F_s}^2}{{F_p}^2} - 17964.96398\frac{F_s}{F_p} + 8508.25346\right) Re_{Dc}^{\left(-835.94824\frac{{F_s}^2}{{F_p}^2}+1579.81844\frac{F_s}{F_p}-746.95346\right)} \quad (2.80)$$

			FCFM-DT				
j factor	Condition	Row	a'	b'	c'	d'	e'
j_h	Fully wet	1	0.841337	0.20121	−0.03333	−0.00997	−0.68104
		2	1.12687	0.047591	−0.0490	−0.0082	−0.54295
		4	0.866876	0.543626	−0.03607	−0.01055	−0.99802
		6	0.62910	0	0	0	−0.54518
	Partially wet	1	0.52917	0	0	0	−0.54109
		2	0.965838	0.710793	−0.06071	0.003429	−1.14855
		4	0.322181	1.205485	−0.07158	0.041929	−1.5616
j_m	Fully wet	1	0.617171	0.224823	−0.05117	0.021837	−0.70229
		2	0.581529	−0.27842	−0.0453	0.013473	−0.21589
		4	0.253784	0.583085	−0.05503	0.024426	−0.92567
		6	0.180675	0	0	0	−0.392667
	Partially wet	1	0.0700053	0	0	0	−0.212952
		2	0.400523	0.681252	−0.0284	−0.01436	−0.9745
		4	0.414881	0.023086	−0.05595	0.040567	−0.48991

Figure 2-7 Plain fin coefficients for jh and jm (Source: [33])

2.5.2.5.2 Herringbone wavy fin

For dry conditions; [34]

For ReDc<1000

$$j = 0.882 {Re_{Dc}}^{J1} \left(\frac{D_c}{D_h}\right)^{J2} \left(\frac{F_s}{P_t}\right)^{J3} \left(\frac{F_s}{D_c}\right)^{-1.58} (tan\theta)^{-0.2} \quad (2.81)$$

$$J1 = 0.0045 - 0.491 {Re_{Dc}}^{-0.0316-0.0171\ln(Ntan\theta)} \left(\frac{P_l}{P_t}\right)^{-0.1019\ln(Ntan\theta)} \left(\frac{D_c}{D_h}\right)^{0.542+0.0471N} \left(\frac{F_s}{D_c}\right)^{0.984} \left(\frac{F_s}{P_t}\right)^{-0.349} \quad (2.82)$$

$$J2 = -2.72 + 6.48tan\theta \tag{2.83}$$

$$J3 = 2.66tan\theta \tag{2.84}$$

			FCFM-DT				
j factor	Condition	Row	a'	b'	c'	d'	e'
j_h	Fully wet	1	0.841337	0.20121	−0.03333	−0.00997	−0.68104
		2	1.12687	0.047591	−0.0490	−0.0082	−0.54295
		4	0.866876	0.543626	−0.03607	−0.01055	−0.99802
		6	0.62910	0	0	0	−0.54518
	Partially wet	1	0.52917	0	0	0	−0.54109
		2	0.965838	0.710793	−0.06071	0.003429	−1.14855
		4	0.322181	1.205485	−0.07158	0.041929	−1.5616
j_m	Fully wet	1	0.617171	0.224823	−0.05117	0.021837	−0.70229
		2	0.581529	−0.27842	−0.0453	0.013473	−0.21589
		4	0.253784	0.583085	−0.05503	0.024426	−0.92567
		6	0.180675	0	0	0	−0.392667
	Partially wet	1	0.0700053	0	0	0	−0.212952
		2	0.400523	0.681252	−0.0284	−0.01436	−0.9745
		4	0.414881	0.023086	−0.05595	0.040567	−0.48991

Figure 2-8 Plain fin coefficients for jh and jm (Source:[33])

$$f = 4.37{Re_{Dc}}^{F1}(\frac{F_s}{D_h})^{F2}(\frac{P_l}{P_t})^{F3}(\frac{D_c}{D_h})^{0.2054}N^{F4} \tag{2.85}$$

$$F1 = -0.574 - 0.137(\ln(Re_{Dc}) - 5.26)^{0.245}\left(\frac{P_t}{D_c}\right)^{-0.765} \left(\frac{D_c}{D_h}\right)^{-0.243}\left(\frac{F_s}{D_h}\right)^{-0.474}(tan\theta)^{-0.217}N^{0.035} \tag{2.86}$$

$$F2 = -3.05tan\theta \tag{2.87}$$

$$F3 = -0.192N \tag{2.88}$$

$$F4 = -0.646tan\theta \tag{2.89}$$

For ReDc≥1000

$$j = 0.0646{Re_{Dc}}^{J1}(\frac{D_c}{D_h})^{J2}(\frac{F_s}{P_t})^{-1.03}(\frac{P_l}{D_c})^{0.432}(tan\theta)^{-0.692}N^{-0.737} \tag{2.90}$$

$$J1 = -0.0545 - 0.0538tan\theta - 0.302N^{-0.24}\left(\frac{F_s}{P_l}\right)^{-1.3} (\frac{P_l}{P_t})^{0.379}(\frac{P_l}{D_h})^{-1.35}tan\theta^{-0.256} \tag{2.91}$$

$$J2 = -1.29(\frac{P_l}{P_t})^{1.77-9.43tan\theta}(\frac{D_c}{D_h})^{0.229-1.43tan\theta}(\frac{F_s}{P_t})^{-0.174\ln(0.5N)}N^{-0.166-1.08tan\theta} \tag{2.92}$$

$$f = 0.228{Re_{Dc}}^{F1}tan\theta^{F2}(\frac{F_s}{P_l})^{F3}(\frac{P_l}{D_c})^{F4}(\frac{D_c}{D_h})^{0.383}(\frac{P_l}{P_t})^{-0.247} \tag{2.93}$$

$$F1 = -0.141(\frac{F_s}{P_l})^{0.0512}(tan\theta)^{-0.472}(\frac{P_l}{P_t})^{0.35}(\frac{P_t}{D_h})^{0.449tan\theta}N^{-0.049+.0237tan\theta} \tag{2.94}$$

$$F2 = -0.562(\ln(Re_{Dc}))^{-0.0923}N^{0.013} \tag{2.95}$$

$$F3 = 0.302{Re_{Dc}}^{0.03}(\frac{P_t}{D_c})^{0.026} \tag{2.96}$$

$$F4 = -0.306 + 3.63tan\theta \tag{2.97}$$

For wet conditions [35]

$$j = 0.472293{Re_{Dc}}^{j1}\left(\frac{P_t}{P_l}\right)^{j2}\left(\frac{P_d}{X_f}\right)^{j3}\left(\frac{P_d}{F_s}\right)^{j4}N^{-0.4933} \tag{2.98}$$

$$f = 0.149001{Re_{Dc}}^{f1}\left(\frac{P_t}{P_l}\right)^{f2}N^{f3}ln\left(3.1 - \frac{P_d}{X_f}\right)^{f4}\left(\frac{F_p}{D_c}\right)^{f5}\left(\frac{2\Gamma}{\mu}\right)^{0.0769} \tag{2.99}$$

Where

$$j1 = -0.5836 + 0.2371\left(\frac{F_s}{D_c}\right)^{0.55} N^{0.34}\left(\frac{P_t}{P_l}\right)^{1.2} \tag{2.100}$$

$$j2 = 1.1873 - 3.0219\left(\frac{F_s}{D_c}\right)^{1.5}\left(\frac{P_d}{X_f}\right)^{0.9}(lnRe_{Dc})^{1.22} \tag{2.101}$$

$$j3 = 0.006672\left(\frac{P_t}{P_l}\right)N^{1.96} \tag{2.102}$$

$$j4 = -0.1157\left(\frac{F_s}{D_c}\right)^{0.9} ln\left(\frac{50}{Re_{Dc}}\right) \tag{2.103}$$

$$f1 = -0.067 + \left(\frac{P_d}{F_s}\right)\left(\frac{1.35 - 0.15N}{\ln\left(Re_{Dc}\right.}\right) + 0.0153\left(\frac{F_s}{D_c}\right) \tag{2.104}$$

$$f2 = 2.981 - 0.082ln(Re_{Dc}) + \left(\frac{0.127N}{4.05 - \ln\left(Re_{Dc}\right)}\right) \tag{2.105}$$

$$f3 = 0.53 - 0.0491ln(Re_{Dc}) \tag{2.106}$$

$$f4 = 11.91\left(\frac{N}{\ln\left(Re_{Dc}\right)}\right)^{0.7} \tag{2.107}$$

$$f5 = 1.32 + 0.287ln(Re_{Dc}) \tag{2.108}$$

Pirompugd and Wong, also [36] published correlations for wavy fin tube heat exchangers according to the actual dry bulb and equivalent dry bulb method. Correlations shown below are for actual dry bulb temperature method.

Under fully wet conditions 1-2-4 rows

$$j = aRe_{Dc}^{\left(b\frac{F_s}{F_p} + c\frac{P_l}{D_c} + d\frac{P_t}{D_c} + e\right)} \tag{2.109}$$

Under fully wet conditions 6 rows and under partially wet conditions 4,6 rows: [37]

$$j = \left(a\frac{F_s}{F_p} + b\right)Re_{Dc}^{\left(c\frac{F_s}{F_p} + d\right)} \tag{2.110}$$

j factor	Condition	Row	ADTM				
			a	*b*	*c*	*d*	*e*
j_h	Fully wet	1	1.05218	−0.7106	−0.00695	−0.01116	0.11703
		2	0.75231	−0.18445	0.05793	−0.09375	−0.25
		4	0.75301	−0.94821	−0.05803	0.5	−1
		6	7.69188	−6.9047	−2.1322	1.5411	–
	Partially wet	1	–	–	–	–	–
		2	–	–	–	–	–
		4	0	0.6197	0	−0.5492	–
		6	0	0.08007	0	−0.3130	–
j_m	Fully wet	1	0.86655	−0.75826	0.18446	−0.17402	0.23174
		2	0.54825	−0.39237	0.02768	0.03125	−0.3125
		4	0.21649	0.52874	0.14902	−0.125	−0.875
		6	22.4884	−21.4529	−35.5661	33.8077	–
	Partially wet	1	–	–	–	–	–
		2	-	–	–	–	–
		4	0	0.17048	0	−0.35606	–
		6	0	0.14096	0	−0.33121	–

Figure 2-9 Wavy fin coefficients for jh and jm (Source:[36])

$300<Re_{Dc}<5000$

N>1 (fully wet conditions)

$$j_{h,N,f} = j_{h,1} N^{-0.06451} \left(\frac{S_p}{D_c}\right)^{(-0.1219N+0.7381)} (\varepsilon)^{(-0.1219N+0.7381)} Re_{Dc}^{\left(0.03475N-0.1145\frac{F_s}{D_c}+0.00521\frac{P_l}{D_c}-0.03498\frac{P_t}{D_c}-0.04374\right)} \quad (2.111)$$

$$j_{m,N,f} = j_{m,1} N^{0.1016} \left(\frac{S_p}{D_c}\right)^{(-0.2419N+2.5353)} (\varepsilon)^{(-0.312N+1.8373)} Re_{Dc}^{\left(0.0654N-0.1935\frac{F_s}{D_c}+0.133\frac{P_l}{D_c}-0.2329\frac{P_t}{D_c}+0.1563\right)} \quad (2.112)$$

$$j_{m,1} = 1.00006 \left(\frac{P_l}{D_c}\right)^{-1.6741} \left(\frac{P_t}{D_c}\right)^{-0.6715} Re_{Dc}^{\left(-0.4252\frac{F_s}{D_c}+0.1398\frac{P_l}{D_c}+0.1408\frac{P_t}{D_c}-0.8472\right)} \quad (2.113)$$

N=1 (fully wet and partially wet conditions)

$$j_{h,1} = 6.6412\left(\frac{P_l}{D_c}\right)^{-0,00085}\left(\frac{P_t}{D_c}\right)^{-2.1461} Re_{Dc}^{\left(-0.2636\frac{F_s}{D_c}-0.00091\frac{P_l}{D_c}+0.1558\frac{P_t}{D_c}-0.8865\right)} \quad (2.114)$$

$$j_{m,1} = 1.00006\left(\frac{P_l}{D_c}\right)^{-1.6741}\left(\frac{P_t}{D_c}\right)^{-0.6715} Re_{Dc}^{\left(-0.4252\frac{F_s}{D_c}+0.1398\frac{P_l}{D_c}+0.1408\frac{P_t}{D_c}-0.8472\right)} \quad (2.115)$$

j factor	Condition	Row	EDTM				
			a'	b'	c'	d'	e'
j_h	Fully wet	1	0.6568	−1.1446	0.01211	0.00832	0.5274
		2	0.6949	−0.06653	0.1254	−0.125	−0.375
		4	5.5261	−4.8321	−1.6842	1.1259	–
		6	7.1009	−6.5440	−10.0817	9.2485	–
	Partially wet	1	–	–	–	–	–
		2	–	–	–	–	–
		4	95.0064	−87.9662	−77.9869	72.0242	–
		6	3.8398	−3.3891	−1.3425	0.8512	–
j_m	Fully wet	1	0.2291	−1.2896	0.01631	0.01674	0.7948
		2	0.1828	−0.5107	0.1022	0.09375	−0.375
		4	0.08262	−0.07478	0.327	−0.3125	0
		6	6.3875	−6.0755	−21.3796	20.3301	–
	Partially wet	1	–	–	–	–	–
		2	–	–	–	–	–
		4	0	0.22129	0	−0.3935	–
		6	13.6255	−12.5429	−9.9958	9.0243	–

Figure 2-10 Wavy fin coefficients for jh and jm (Source:[36])

N>1 (partially wet conditions 65% <A_{wet}/A_o <100%)

$$j_{h,N,p} = j_{h,N,f} N^{-1.7838}\left(\frac{S_p}{D_c}\right)^{(-0.9459N+3.9329)} \left(\frac{A_{wet}}{A_o}\right)^{(0.6919N-4.7697)} Re_{Dc}^{\left(-0.1554N+1.1667\frac{F_s}{D_c}+0.2253\frac{P_l}{D_c}-0.1645\frac{P_t}{D_c}+0.7158\right)} \quad (2.116)$$

$$j_{m,N,p} = j_{m,N,f} N^{-1.6415}\left(\frac{S_p}{D_c}\right)^{(-0.7655N+4.0144)} \left(\frac{A_{wet}}{A_o}\right)^{(1.16N-7.793)} Re_{Dc}^{\left(-0.1151N+0.695\frac{F_s}{D_c}+0.5492\frac{P_l}{D_c}-0.4798\frac{P_t}{D_c}+0.974\right)} \quad (2.117)$$

2.5.2.5.3 Louver fin

Dry conditions [29]

Flat tube

$$j = {Re_{Lp}}^{-0.49}\left(\frac{\theta}{90}\right)^{0.27}\left(\frac{F_p}{L_p}\right)^{-0.14}(\frac{F_l}{L_p})^{-0.29}(\frac{T_d}{L_p})^{-0.23}(\frac{L_l}{L_p})^{0.68}(\frac{T_p}{L_p})^{-0.28}(\frac{t_{fin}}{L_p})^{-0.05} \quad (2.118)$$

Round tube

For Re_{Dc}<1000

$$j = 14.3117{Re_{Dc}}^{J1}(\frac{F_p}{D_c})^{J2}(\frac{L_h}{L_p})^{J3}(\frac{F_p}{P_l})^{J4}(\frac{P_l}{P_t})^{-1.724} \quad (2.119)$$

$$J1 = -0.991 - 0.1055\left(\frac{P_l}{P_t}\right)^{3.1}\ln(\frac{L_h}{L_p}) \quad (2.120)$$

$$J2 = -0.7344 + 2.1059(\frac{N^{0.55}}{\ln(Re_{Dc}) - 3.2}) \quad (2.121)$$

$$J3 = 0.08485\left(\frac{P_l}{P_t}\right)^{-4.4}N^{-0.68} \quad (2.122)$$

$$J4 = -0.1741\ln(N) \quad (2.123)$$

For ReDc≥1000

$$j = 1.1373{Re_{Dc}}^{J1}\left(\frac{F_p}{P_l}\right)^{J2}\left(\frac{L_h}{L_p}\right)^{J3}\left(\frac{P_l}{P_t}\right)^{J4}(N)^{0.3545} \quad (2.124)$$

$$J1 = -0.6027 - 0.02593\left(\frac{P_l}{D_{ht}}\right)^{0.52}\ln\left(\frac{L_h}{L_p}\right)N^{-0.5} \quad (2.125)$$

$$J2 = -0.4776 + 0.40774\left(\frac{N^{0.7}}{\ln(Re_{Dc}) - 4.4}\right) \quad (2.126)$$

$$J3 = -0.58655\left(\frac{F_p}{D_h}\right)^{2.3}\left(\frac{P_l}{P_t}\right)^{-1.6}N^{-0.65} \tag{2.127}$$

$$J4 = 0.0814(\ln(Re_{Dc}) - 3) \tag{2.128}$$

Wet conditions [38]

$$j = 9.717{Re_{Dc}}^{j1}\left(\frac{F_p}{D_c}\right)^{j2}\left(\frac{P_l}{P_t}\right)^{j3} ln\left(3 - \frac{L_p}{F_p}\right)^{0.07162} N^{-0.543} \tag{2.129}$$

$$j_1 = -0.023634 - 1.2475\left(\frac{F_p}{D_c}\right)^{0.65}\left(\frac{P_l}{P_t}\right)^{0.2} N^{-0.18} \tag{2.130}$$

$$j_2 = 0.856\exp\left(tan\theta_l\right) \tag{2.131}$$

$$\theta_l = \frac{L_h}{L_p} \tag{2.132}$$

$$j_3 = 0.25ln(Re_{Dc}) \tag{2.133}$$

$$f = 2.814{Re_{Dc}}^{f1}\left(\frac{F_p}{D_c}\right)^{f2}\left(\frac{P_l}{D_c}\right)^{f3}\left(\frac{P_l}{P_t} + 0.091\right)^{f4}\left(\frac{L_p}{F_p}\right)^{1.958} N^{0.04674} \tag{2.134}$$

$$f_1 = 1.223 - 2.857\left(\frac{F_p}{D_c}\right)^{0.71}\left(\frac{P_l}{P_t}\right)^{-0.05} \tag{2.135}$$

$$f_2 = 0.8079ln(Re_{Dc}) \tag{2.136}$$

$$f_3 = 0.8932ln(Re_{Dc}) \tag{2.137}$$

$$f_4 = -0.999ln\left(\frac{2\Gamma}{\mu_f}\right) \tag{2.138}$$

General friction coefficient for louver fin geometry

$$f = f_1 f_2 f_3 \tag{2.139}$$

For Re_{Lp}<150

$$f_1 = 1.39 Re_{Lp}^{\left(-\frac{0.805F_p}{F_1}\right)} \left(\ln\left(1+\left(\frac{F_p}{L_p}\right)\right)\right)^{3.04} \tag{2.140}$$

$$f_2 = \left(ln\left(\left(\frac{F_t}{F_p}\right)^{0.48} + 0.9\right)\right)^{-1.435} \left(\frac{D_h}{L_p}\right)^{-3.01} \left(ln(0.5Re_{Lp})\right)^{-3.01} \tag{2.141}$$

$$f_3 = \left(\frac{F_p F_d}{{L_1}^2}\right)^{-0.308} \left(e^{-0.1167\frac{T_p}{D_m}}\right) {\theta_l}^{0.35} \tag{2.142}$$

For 150<Re_{Lp}<5000

$$f_1 = 4.97 Re_{Lp}^{\left(0.6049-\frac{1.064}{\theta^{0.2}}\right)} \left(\ln\left(\left(\frac{F_t}{F_p}\right)^{0.5} + 0.9\right)\right)^{-0.527} \tag{2.143}$$

$$f_2 = \left(\left(\frac{D_h}{L_p}\right) ln(0.3Re_{Lp})\right)^{-2.966} \left(\frac{F_p}{L_1}\right)^{-0.7931\left(\frac{T_p}{T_h}\right)} \tag{2.144}$$

$$f_3 = \left(\frac{T_p}{D_m}\right)^{-0.0446} \left(ln\left(1.2+\left(\frac{L_p}{F_p}\right)^{1.4}\right)\right)^{-3.553} {\theta_l}^{-0.477} \tag{2.145}$$

2.5.2.5.4 Slit fin

Dry conditions [29]

$$j = 5.98 {Re_{Dc}}^{j1} \left(\frac{F_s}{D_c}\right)^{j2} N^{j3} \left(\frac{S_s}{S_h}\right)^{j4} \left(\frac{P_t}{P_l}\right)^{0.804} \tag{2.146}$$

$$f = 0.1851 {Re_{Dc}}^{f1} \left(\frac{F_s}{D_c}\right)^{f2} \left(\frac{S_s}{S_h}\right)^{f3} N^{-0.046} \tag{2.147}$$

$$j_1 = -0.647 + 0.198\frac{N}{ln(Re_{Dc})} - 0.458\frac{F_s}{D_c} + 2.52\frac{N}{Re_{Dc}} \tag{2.148}$$

$$j_2 = 0.116 + 1.125\frac{N}{ln(Re_{Dc})} - 47.6\frac{N}{Re_{Dc}} \quad (2.149)$$

$$j_3 = 0.49 + 175\frac{\frac{F_s}{D_c}}{Re_{Dc}} - \frac{3.08}{ln(Re_{Dc})} \quad (2.150)$$

$$j_4 = 0.63 + 0.086S_n \quad (2.151)$$

$$f_1 = -1.485 + 0.656\left(\frac{F_s}{D_c}\right) + 0.855\left(\frac{P_t}{P_l}\right) \quad (2.152)$$

$$f_2 = -1.04 - \frac{125}{Re_{Dc}} \quad (2.153)$$

$$f_3 = -0.83 + 0.117S_n \quad (2.154)$$

Wet conditions [39]

$$j = 0.7291{Re_{Dc}}^{j1}\left(\frac{P_t}{P_l}\right)^{0.188} N^{0.0218}\left(\frac{S_s}{S_h}\right)^{-0.0671} {S_n}^{0.1937} \quad (2.155)$$

$$f = 0.501{Re_{Dc}}^{f1}\left(\frac{F_s}{D_c}\right)^{f2}\left(\frac{P_t}{P_l}\right)^{-1.1858} N^{0.06}\left(\frac{S_s}{S_h}\right)^{-0.07162} \quad (2.156)$$

$$j_1 = -0.5264 - \frac{0.0456}{\left(1 + \frac{2\Gamma}{\mu_f}\right)^2} - 0.0003N^3 \quad (2.157)$$

$$f_1 = -0.3021 + \frac{3.2065}{\sqrt{Re_{Dc}}} + 0.0844\frac{\ln\left(1 + \frac{2\Gamma}{\mu_f}\right)}{1 + \frac{2\Gamma}{\mu_f}} \quad (2.158)$$

$$f_2 = -0.2756 - 0.0044lnRe_{Dc} - 0.0013\left(\frac{F_s}{D_c}\right) \quad (2.159)$$

2.5.2.6 Refrigerant side heat transfer correlations

In the literature, there are many studies on refrigerant side heat transfer and pressure drop correlations. In this section, correlations will be explained to implement segment by segment method. Correlations are examined according to the refrigerant phase change procedure in horizontal smooth tubes.

Two phase examinations are the most complex part for heat exchanger calculations. While a lot of overall refrigerant heat transfer calculations are enough for tube by tube methods, for segment by segment method, refrigerant phase changing conditions in two phase region are getting more complex.

2.5.2.6.1 Two Phase Condensation

Thome et al. [40] developed a new flow pattern map for refrigerant condensation in horizontal tubes. According to this method, new regions are introduced for refrigerant flow name, fully-stratified (S), stratified wavy (SW), intermittent (I), annular (A), mist (MF) and bubbly(B) flow. Thome et al. calculated transition mass flow velocities for each region to decide the flow regimes. Ranges for flow pattern is shown below.

Annular flow

$G>G_{wavy}$, $G<G_{mist}$ or $G<G_{bubbly}$ and $x<x_{IA}$

Intermittent flow

$G>G_{wavy}$, $G<G_{mist}$ and $x>x_{IA}$

Stratified wavy flow

$G_{strat}<G<G_{wavy}$

Fully stratified flow

$G<G_{strat}$

Mist flow

$G>G_{mist}$

Calculations are given below respect to the calculation order.

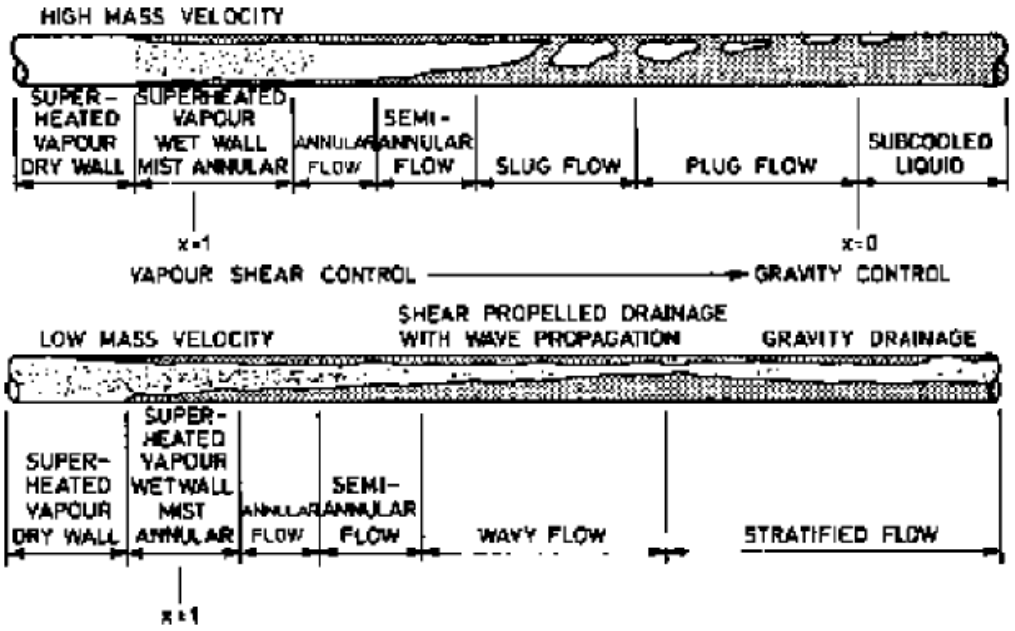

Figure 2-11 Two phase flow patterns in horizontal tube according (Source:[40])

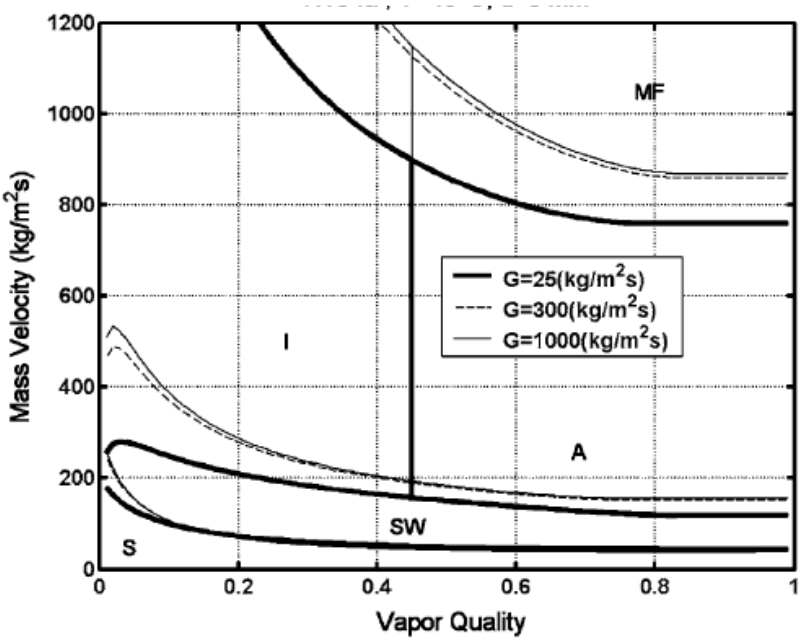

Figure 2-12 R134 a at 40C inner diameter 8mm mass flow pattern according to the vapor quality and mass flow velocity (Source:[40])

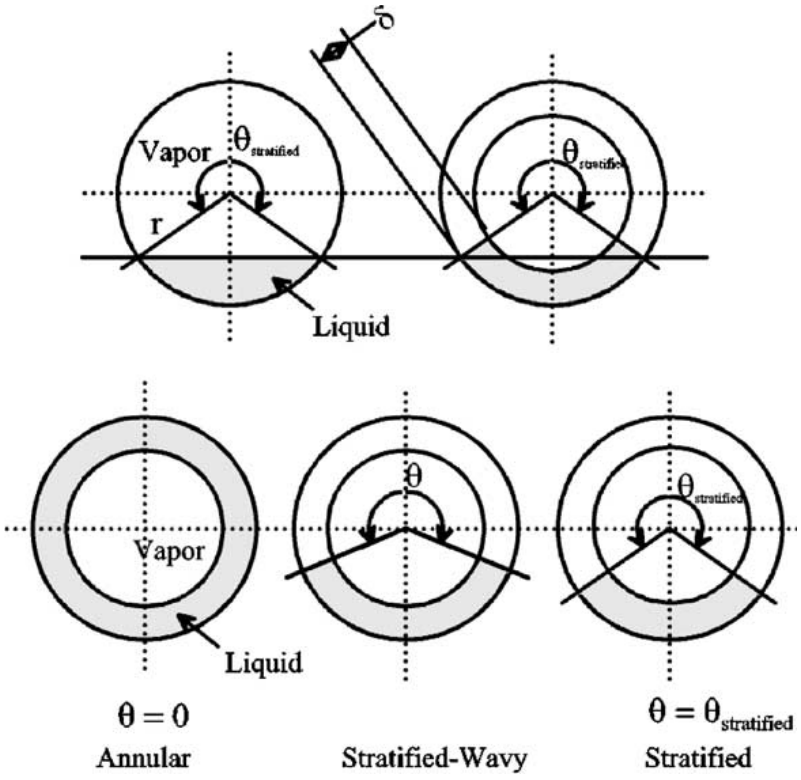

Figure 2-13 Dry angle positions according to flow pattern (Source:[41])

$$\varepsilon_h = \left(1 + \left(\frac{1-x}{x}\right)\left(\frac{\rho_V}{\rho_L}\right)\right)^{-1} \tag{2.160}$$

$$\varepsilon_{ra} = \frac{x}{\rho_V}\left([1 + 0.12(1-x)]\left[\frac{x}{\rho_V} + \frac{1-x}{\rho_L}\right] + \frac{1.18(1-x)[g\sigma(\rho_L - \rho_V)]^{0.25}}{G{\rho_L}^{0.5}}\right)^{-1} \tag{2.161}$$

$$\varepsilon_{vv} = \frac{\varepsilon_h - \varepsilon_{ra}}{ln\left(\frac{\varepsilon_h}{\varepsilon_{ra}}\right)} \tag{2.162}$$

$$\theta_{strat} = 2\pi - 2\left\{\pi(1-\varepsilon_{vv}) + \left(\frac{3\pi}{2}\right)^{1/3}\left[1 - 2(1-\varepsilon_{vv}) + (1-\varepsilon_{vv})^{\frac{1}{3}} - {\varepsilon_{vv}}^{1/3}\right] - \frac{1}{200}(1-\varepsilon_{vv})\varepsilon_{vv}[1-2(1-\varepsilon_{vv})][1+4((1-\varepsilon_{vv})^2 + {\varepsilon_{vv}}^2)]\right\} \tag{2.163}$$

$$\left(\frac{We}{Fr}\right)_L = \frac{g{d_i}^2\rho_L}{\sigma} \tag{2.164}$$

$$A_{Ld} = \frac{1}{8}[(2\pi - \theta_{strat}) - sin(2\pi - \theta_{strat})] \tag{2.165}$$

$$A_L = \mathrm{A}_i(1 - \varepsilon_{vv}) \tag{2.166}$$

$$A_v = A\varepsilon_{vv} \tag{2.167}$$

$$A_{vd} = \frac{A_v}{{d_{in}}^2} \tag{2.168}$$

$$P_{id} = sin\left(\frac{2\pi - \theta_{strat}}{2}\right) \tag{2.169}$$

$$h_{Ld} = 0.5\left(1 - \cos\left(\frac{2\pi - \theta_{strat}}{2}\right)\right) \tag{2.170}$$

$$\xi = \left[1.138 + 2log\left(\frac{\pi}{1.5A_{Ld}}\right)\right]^{-2} \tag{2.171}$$

$$G_{wavy} = \left\{\frac{16{A_{vd}}^3 g d_i \rho_L \rho_V}{x^2\pi^2(1-(2h_{Ld}-1)^2)^{0.5}}\left[\frac{\pi^2}{25{h_{Ld}}^2}\left(\frac{We}{Fr}\right)_L^{-1.023} + 1\right]\right\}^{0.5} + 50 - 75e^{-\left(x^2-0.97\right)^2/x(1-x)} \tag{2.172}$$

$$G_{strat} = \left\{\frac{(226.3)^2 A_{Ld}{A_{vd}}^2 \rho_v(\rho_L - \rho_v)\mu_L g}{x^2(1-x)\pi^3}\right\} + 20x \tag{2.173}$$

$$G_{mist} = \left\{\frac{7680{A_{vd}}^2 g d_i \rho_L \rho_v}{x^2\pi^2\xi}\left(\frac{Fr}{We}\right)_L\right\}^{0.5} \tag{2.174}$$

$$G_{bubbly} = \left\{\frac{256A_{Vd}{A_{Ld}}^2 {d_{in}}^{1.25}\rho_L(\rho_L - \rho_V)g}{0.3164(1-x)^{1.75}\pi^2 P_{id}{\mu_L}^{0.25}}\right\}^{1/1.75} \tag{2.175}$$

$$x_{IA} = \left\{\left[0.2914\left(\frac{\rho_V}{\rho_L}\right)^{-1/1.75}\left(\frac{\mu_L}{\mu_V}\right)^{-1/7}\right] + 1\right\}^{-1} \tag{2.176}$$

$$\delta = \frac{d_i}{2} - \sqrt{\left(\frac{d_i}{2}\right)^2 - \frac{2A_l}{(2\pi - \theta_{dry})}} \tag{2.177}$$

If δ>d/2 δ=d/2

$$Re_L = \frac{4G(1-x)\delta}{(1-\varepsilon)\mu_L} \tag{2.178}$$

$$Pr_L = \frac{C_{pL}\mu_L}{k_L} \tag{2.179}$$

For Annular, intermittent and mist flow

$$\theta_{dry} = 0 \tag{2.180}$$

$$f_i = 1 + \left(\frac{u_V}{u_L}\right)^{1/2}\left(\frac{(\rho_L - \rho_V)g\delta^2}{\sigma}\right)^{1/4} \tag{2.181}$$

For the stratified wavy flow

$$\theta_{dry} = \theta_{strat} \tag{2.182}$$

$$f_i = 1 + \left(\frac{u_V}{u_L}\right)^{1/2}\left(\frac{(\rho_L - \rho_V)g\delta^2}{\sigma}\right)^{1/4}\left(\frac{G}{G_{strat}}\right) \tag{2.183}$$

Fully stratified wavy

$$\theta_{dry} = \theta_{strat}\left[\frac{(G_{wavy} - G)}{(G_{wavy} - G_{strat})}\right]^{0.5} \tag{2.184}$$

$$f_i = 1 + \left(\frac{u_V}{u_L}\right)^{1/2}\left(\frac{(\rho_L - \rho_V)g\delta^2}{\sigma}\right)^{1/4}\left(\frac{G}{G_{strat}}\right) \tag{2.185}$$

$$h_c = 0.003{Re_L}^{0.74}{Pr_L}^{0.5}\frac{k_L}{\delta}f_i \tag{2.186}$$

$$h_f = 0.655\left[\frac{\rho_L(\rho_L - \rho_V)gh_{LV}{k_L}^3}{\mu_L d_i q}\right]^{1/3} \tag{2.187}$$

$$h_{tp} = \frac{h_f r\theta + (2\pi - \theta_{dry})rh_c}{2\pi r} \tag{2.188}$$

2.5.2.6.2 Two Phase Evaporation

Similarly to condensation, evaporation flow patterns are developed by J.R.Thome and his team mates. Furthermore, in this case some flow patterns are added. The flow pattern names are respectively, Slug (S), Slug + stratified wavy (SSW), Stratified wavy (SW), Intermittent (I), Annular (A), Dryout (D) and Mist (M) flow [42]. Once more, the transition mass flow velocities designate the flow pattern conditions.

The zone is distinguished by the flow pattern as;

Slug zone

If $G_{wavy,xIA}<G$ and $G_{wavy}>G$

Slug+stratified wavy zone

if $G_{strat}<G<G_{wavy,xIA}$ and $x<x_{IA}$ and $G_{wavy}>G$

Stratified wavy zone

if $x \geq x_{IA}$ and $G_{wavy}>G$

Intermittent

if $G>G_{wavy}$ and $G<G_{dryout}$ and $x<x_{IA}$

Annular

if $G>G_{wavy}$ and $G<G_{dryout}$ and $x> x_{IA}$

Dryout

if $G_{mist}>G>G_{dryout}$

Mist

if $G > G_{mist}$

Calculations are given below in respect to the calculation order. [43]

$$G_{dry,out} = \left[\frac{\frac{1}{0.235}\left(ln\left(\frac{0.58}{x}\right)+0.52\right)\left(\frac{d_i}{\rho_V \sigma}\right)^{-0.17}}{\left(\frac{1}{g d_i \rho_V (\rho_L - \rho_V)}\right)^{-0.37}\left(\frac{\rho_V}{\rho_L}\right)^{-0.25}\left(\frac{q}{\rho_{crit}}\right)^{-0.7}} \right]^{0.926} \tag{2.189}$$

$$G_{mist} = \left[\frac{\frac{1}{0.0058}\left(ln\left(\frac{0.61}{x}\right)+0.57\right)\left(\frac{d_i}{\rho_V \sigma}\right)^{-0.38}}{\left(\frac{1}{g d_{in} \rho_V (\rho_L - \rho_V)}\right)^{-0.15}\left(\frac{\rho_V}{\rho_L}\right)^{0.09}\left(\frac{q}{\rho_{crit}}\right)^{-0.27}} \right]^{0.943} \tag{2.190}$$

$$G_{wavy} = \left\{ \frac{16{A_{vd}}^3 g d_i \rho_L \rho_v}{x^2 \pi^2 (1-(2h_{Ld}-1)^2)^{0.5}} \left[\frac{\pi^2}{25{h_{Ld}}^2} \left(\frac{We}{Fr}\right)_L^{-1} + 1 \right] \right\}^{0.5} + 50 \tag{2.191}$$

$$G_{strat} = \left\{ \frac{(226.3)^2 A_{Ld} {A_{vd}}^2 \rho_v (\rho_L - \rho_v) \mu_L g}{x^2 (1-x) \pi^3} \right\} \tag{2.192}$$

$$x_{IA} = \left\{ \left[0.2914 \left(\frac{\rho_V}{\rho_L}\right)^{-1/1.75} \left(\frac{\mu_L}{\mu_V}\right)^{-1/7} \right] + 1 \right\}^{-1} \tag{2.193}$$

$$\theta_{strat} = 2\pi - 2\left\{ \pi(1-\varepsilon_{vv}) + \left(\frac{3\pi}{2}\right)^{\frac{1}{3}} \left[1 - 2(1-\varepsilon_{vv}) + (1-\varepsilon_{vv})^{\frac{1}{3}} - e{\varepsilon_{vv}}^{\frac{1}{3}} \right] - \frac{1}{200}(1-\varepsilon_{vv})\varepsilon_{vv}[1-2(1-\varepsilon_{vv})][1+4((1-\varepsilon_{vv})^2 + {\varepsilon_{vv}}^2)] \right\} \tag{2.194}$$

$$\varepsilon_h = \left(1 + \left(\frac{1-x}{x}\right)\left(\frac{\rho_V}{\rho_L}\right) \right)^{-1} \tag{2.195}$$

$$\varepsilon_{ra} = \frac{x}{\rho_v} \left([1 + 0.12(1-x)] \left[\frac{x}{\rho_v} + \frac{1-x}{\rho_L} \right] + \frac{1.18(1-x)[g\sigma(\rho_L - \rho_v)]^{0.25}}{G{\rho_L}^{0.5}} \right)^{-1} \tag{2.196}$$

$$\varepsilon_{vv} = \frac{\varepsilon_h - \varepsilon_{ra}}{ln\left(\frac{\varepsilon_h}{\varepsilon_{ra}}\right)} \tag{2.197}$$

For Slug, intermittent and annular zone

$$\theta_{dry} = 0 \tag{2.198}$$

For stratified

$$\theta_{dry} = \left[\frac{G_{wavy} - G}{G_{wavy} - G_{strat}} \right]^{0.61} \tag{2.199}$$

For SW

$$\theta_{dry} = \left[\frac{G_{wavy} - G}{G_{wavy} - G_{strat}} \right]^{0.61} \theta_{strat} \tag{2.200}$$

For Slug + Sw

$$\theta_{dry} = \frac{x}{x_{IA}}\left[\frac{G_{wavy} - G}{G_{wavy} - G_{strat}}\right]^{0.61} \theta_{strat} \tag{2.201}$$

$$\delta = \frac{d_i}{2} - \sqrt{\left(\frac{d_i}{2}\right)^2 - \frac{2A_L}{\left(2\pi - \theta_{dry}\right)}} \tag{2.202}$$

If δ>d/2 δ=d/2

$$h_{tp} = \frac{\theta_{dry} h_V + \left(2\pi + \theta_{dry}\right) h_{wet}}{2\pi} \tag{2.203}$$

$$h_V = 0.023 {Re_V}^{0.8} {Pr_V}^{0.4} \frac{k_V}{d_i} \tag{2.204}$$

$$h_{cb} = 0.0133 {Re_\delta}^{0.69} {Pr_L}^{0.4} \frac{k_L}{\delta} \tag{2.205}$$

$$h_{nb} = 55(P_r)^{0.12} - (-logP_r)^{-0.55} M^{-0.5} q^{0.67} \tag{2.206}$$

$$h_{wet} = [(h_{cb})^3 + (h_{nb})^3]^{1/3} \tag{2.207}$$

For mist flow

$$Re_H = \frac{G d_i}{\mu_V}\left(x + \frac{\rho_V}{\rho_L}(1 - x)\right) \tag{2.208}$$

$$Y = 1 - 0.1\left[\left(\frac{\rho_L}{\rho_V} - 1\right)(1 - x)\right]^{0.4} \tag{2.209}$$

$$h_{mist} = 0.0117 {Re_H}^{0.79} {Pr_V}^{-1.06} Y^{-1.83} \frac{k_V}{D} \tag{2.210}$$

For dry out

$$q_{crit} = 0.131 {\rho_V}^{0.5} h_{LV} (g(\rho_L - \rho_V)\sigma)^{0.25} \tag{2.211}$$

$$x_{di} = 0.58 e^{\left[0.52 - 0.235 {We_V}^{0.17} {Fr_V}^{0.37} \left(\frac{\rho_V}{\rho_L}\right)^{0.25} \left(\frac{q}{q_{crit}}\right)^{0.7}\right]} \tag{2.212}$$

$$x_{de} = 0.61e^{\left[0.57-0.0058We_V{}^{0.38}Fr_V{}^{0.15}\left(\frac{\rho_V}{\rho_L}\right)^{-0.09}\left(\frac{q}{q_{crit}}\right)^{0.27}\right]} \quad (2.213)$$

$$h_{dryout} = h_{tp}(x_{di}) - \frac{x - x_{di}}{x_{de} - x_{di}}\left[h_{tp}(x_{di}) - h_{mist}(x_{de})\right] \quad (2.214)$$

2.5.2.6.3 For single phase

Single phase calculations in evaporator and condenser are the same as given by the Gnielinski method [44]. In this case, refrigerant properties should be adjusted according to the refrigerant position either in superheated region or subcooled region. Calculations are given below.

If refrigerant is in subcooled region:

Pr_{ref}=Pr_L and k_{ref}=k_L

If Refrigerant is in superheated region:

Pr_{ref}=Pr_V and k_{ref}=k_V

$$h_{sp} = \frac{(Re_{Din} - 1000)Pr_{ref}\left(\frac{f}{2}\right)k_{ref}}{1 + 12.7\sqrt{f/2}\left(Pr_{ref}{}^{0.67} - 1\right)d_{in}} \quad (2.215)$$

$$f = [1.58ln(Re_{Din}) - 3.28]^{-2} \quad (2.216)$$

2.5.2.7 Refrigerant side pressure drop correlations

Refrigerant side pressure drop calculations are divided into three parts, frictional, acceleration and gravitational [6]. Frictional part is the most dominant part in calculations. While gravitational part is for change at elevation in heat exchanger, gravity effect is more dominant in low quality.

$$\Delta P_{ref} = \Delta P_{fric} + \Delta P_{accel} + \Delta P_{grav} \quad (2.217)$$

2.5.2.7.1 Accelerational pressure drop

Accelerational pressure drop calculations are based on the inlet and outlet conditions in tube. Because of that, at single phase region, subcooled and superheated area momentum term is always positive, which means pressure increasing.

For single phase

$$\Delta P_{accel} = {G_{ref}}^2 \left(\frac{1}{\rho_{ref,in}} - \frac{1}{\rho_{ref,out}} \right) \tag{2.218}$$

For two phase

$$\Delta \mathrm{P_{accel}} = {\mathrm{G_{ref}}}^2 \left(\frac{\mathrm{x}^2}{\alpha \rho_{\mathrm{V}}} + \frac{(1-\mathrm{x})^2}{(1-\alpha)\rho_{\mathrm{L}}} \right) \tag{2.219}$$

For void fraction calculations, usually Zivi's [45] formula is being used.

$$\alpha = \frac{1}{1 + \frac{1-\mathrm{x}}{\mathrm{x}} \left(\frac{\rho_{\mathrm{V}}}{\rho_{\mathrm{L}}} \right)^{2/3}} \tag{2.220}$$

2.5.2.7.2 Gravitational pressure drop

Gravitational pressure drop is for elevation difference for the refrigerant. Elevation difference occurs only in tube bends. [6]

$$\Delta P_{grav} = \rho_{ref} g L_{seg} \frac{H_{coil}}{L_{coil}} \tag{2.221}$$

2.5.2.7.3 Frictional pressure drop

Frictional term is the most dominant section of the pressure drop calculations. As for single phase Ragazzi and Pederson approach is shown below, for two phase calculations Thome et al. [46] approach is described.

2.5.2.7.3.1 For single phase

Single phase calculations are given below, according to turbulent and laminar flow, also for vapor and liquid refrigerants.

If $Re_{Din} \leq 2300$

$$f_{ref,V} = f_{ref,L} = \frac{16}{Re_{d,in}} \tag{2.222}$$

If $100{,}000 \geq Re_{Din} \geq 2300$

For vapor refrigerant

$$f_{ref,V} = \frac{0.046}{\left(Re_{d,in}\right)^{0.2}} \tag{2.223}$$

For liquid refrigerant

$$f_{ref,L} = \frac{0.079}{\left(Re_{d,in}\right)^{0.25}} \tag{2.224}$$

If $Re_{Din} \geq 100{,}000$

$$f_{ref,V} = f_{ref,L} = \frac{0.0032 + 0.221\left(Re_{d,in}\right)^{-0.237}}{4} \tag{2.225}$$

Frictional pressure-drop for vapor and liquid:

$$\Delta P_{f,L} = \frac{2 f_L G^2 L}{d_i \rho_{ref}} \tag{2.226}$$

$$\Delta P_{f,V} = \frac{2 f_V G^2 L}{d_i \rho_{ref}} \tag{2.227}$$

2.5.2.7.3.2 Two phase evaporation frictional pressure drop

For two phase calculations are similar to evaporation heat transfer coefficients. Again,

flow pattern method is used by Thome et al. Refrigerant flow positions are similar to evaporation heat transfer coefficients.

Annular flow

$$u_V = \frac{G}{\rho_V}\frac{x}{\varepsilon_{vv}} \tag{2.228}$$

$$u_L = \frac{G}{\rho_L}\frac{1-x}{1-\varepsilon_{vv}} \tag{2.229}$$

$$We_L = \frac{\rho_L {u_L}^2 d_i}{\sigma} \tag{2.230}$$

$$f_{i,anular} = 0.67\left[\frac{\delta}{d_i}\right]^{1.2}\left[\frac{(\rho_L-\rho_V)g\delta^2}{\sigma}\right]^{-0.4}\left(\frac{\mu_V}{\mu_L}\right)^{0.08}(We_L)^{-0.034} \tag{2.231}$$

$$\Delta P_{annular,f} = 4f_{i,anular}\left(\frac{L}{d_i}\right)\frac{\rho_V {u_V}^2}{2} \tag{2.232}$$

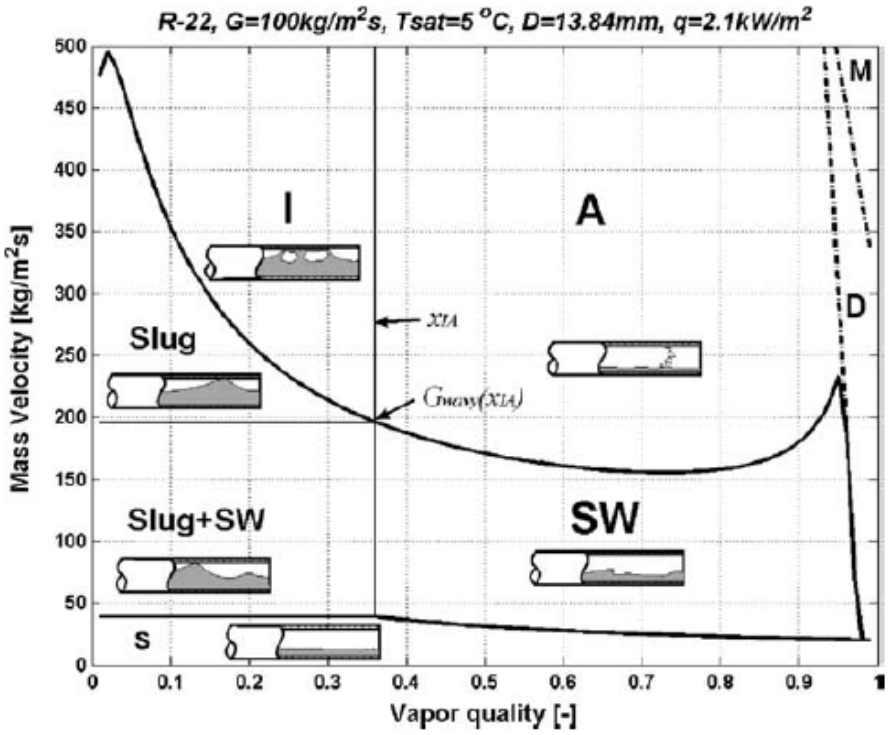

Figure 2-14 Flow pattern map evaluated for R-22 (Source:[40])

Slug + Intermittent flow

$$\varepsilon_h = \left(1 + \left(\frac{1-x}{x}\right)\left(\frac{\rho_V}{\rho_L}\right)\right)^{-1} \tag{2.233}$$

$$\varepsilon_{ra} = \frac{x}{\rho_v}\left([1 + 0.12(1-x)]\left[\frac{x}{\rho_v} + \frac{1-x}{\rho_L}\right] + \frac{1.18(1-x)[g\sigma(\rho_L - \rho_v)]^{0.25}}{G{\rho_L}^{0.5}}\right)^{-1} \tag{2.234}$$

$$\varepsilon_{vv} = \frac{\varepsilon_h - \varepsilon_{ra}}{ln\left(\frac{\varepsilon_h}{\varepsilon_{ra}}\right)} \tag{2.235}$$

$$\Delta P_{slug+intermittent,f} = \Delta P_{f,L}\left(1 - \frac{\varepsilon_{vv}}{\varepsilon_{vv,xIA}}\right)^{0.25} + \Delta P_{annular}\left(\frac{\varepsilon_{vv}}{\varepsilon_{vv,IA}}\right)^{0.25} \tag{2.236}$$

Stratified wavy flow

$${\theta_{dry}}^* = \frac{\theta_{dry}}{2\pi} \tag{2.237}$$

$$Re_G = \frac{Gxd_i}{\mu_V \varepsilon_{vv}} \tag{2.238}$$

$$f_{tp,stratifiedwavy} = {\theta_{dry}}^* \Delta P_{f,V} + \left(1 - {\theta_{dry}}^*\right) f_{i,anular} \tag{2.239}$$

$$\Delta P_{stratifiedwavy,f} = 4 f_{tp,stratifiedwavy}\left(\frac{L}{d_i}\right)\frac{\rho_G {u_G}^2}{2} \tag{2.240}$$

Slug + Stratified wavy flow

$$\Delta P_{slug+stratifiedwavy,f} = \Delta P_{f,L}\left(1 - \frac{\varepsilon_{vv}}{\varepsilon_{vv,IA}}\right)^{0.25} + \Delta P_{stratifiedwavy,f}\left(\frac{\varepsilon_{vv}}{\varepsilon_{vv,IA}}\right)^{0.25} \tag{2.241}$$

Mist flow

$$\varepsilon_H = \frac{1}{1 + \frac{1-x}{x}\frac{\rho_V}{\rho_L}} \tag{2.242}$$

$$\mu_m = x\mu_V + (1-x)\mu_L \tag{2.243}$$

$$Re_m = \frac{Gd_i}{\mu_m} \tag{2.244}$$

$$\rho_m = \rho_L(1-\varepsilon_H) + \rho_g \varepsilon_H \tag{2.245}$$

$$\Delta P_{mist,f} = 2\Delta P_{sp,f,m}\left(\frac{L}{d_i}\right)\frac{G^2}{\rho_m} \tag{2.246}$$

Dryout Flow

$$\mu_{m,xde} = x_{de}\mu_V + (1-x_{de})\mu_L \tag{2.247}$$

$$Re_H = \frac{G d_i}{\mu_{m,xde}} \tag{2.248}$$

$$\Delta P_{mist,f*} = 2\Delta P_{sp,f,m,xde}\left(\frac{L}{d_i}\right)\frac{G^2}{\rho_m} \tag{2.249}$$

$$u_V = \frac{G}{\rho_V}\frac{x_{di}}{\varepsilon_{vv}} \tag{2.250}$$

$$u_L = \frac{G}{\rho_L}\frac{1-x_{di}}{1-\varepsilon_{vv}} \tag{2.251}$$

$$We_{L,xdi} = \frac{\rho_L {u_L}^2 d_i}{\sigma} \tag{2.252}$$

$$f_{i,anular*} = 0.67\left[\frac{\delta}{d_i}\right]^{1.2}\left[\frac{(\rho_L-\rho_V)g\delta^2}{\sigma}\right]^{-0.4}\left(\frac{\mu_V}{\mu_L}\right)^{0.08}\left(We_{L,xdi}\right)^{-0.034} \tag{2.253}$$

$$\Delta P_{annular,f*} = 4 f_{i,anular*}\left(\frac{L}{d_i}\right)\frac{\rho_G {u_G}^2}{2} \tag{2.254}$$

$$\Delta P_{dryout,f} = \Delta P_{annular,f*} - \frac{x-x_{di}}{x_{de}-x_{di}}\left(\Delta P_{annular,f*} - \Delta P_{mist,f*}\right) \tag{2.255}$$

Stratified flow

$${\theta_{strat}}^* = \frac{\theta_{strat}}{2\pi} \tag{2.256}$$

$$f_{tp,stratified} = {\theta_{strat}}^*\Delta P_{sp,f,V} + (1-{\theta_{strat}}^*) f_{i,anular} \tag{2.257}$$

$$u_V = \frac{G}{\rho_V}\frac{x}{\varepsilon_{vv}} \tag{2.258}$$

$$\Delta P_{stratified,1} = 4 f_{tp,stratified}\left(\frac{L}{d_i}\right)\frac{\rho_V {u_V}^2}{2} \tag{2.259}$$

If $x \geq x_{IA}$

$$\Delta P_{stratified,f} = \Delta P_{stratified,1} \tag{2.260}$$

If $x < x_{IA}$

$$\Delta P_{stratified,f} = \Delta P_{f,L}\left(1 - \frac{\varepsilon_{vv}}{\varepsilon_{vv,IA}}\right)^{0.25} + \Delta P_{stratified,1}\left(\frac{\varepsilon_{vv}}{\varepsilon_{vv,IA}}\right)^{0.25} \tag{2.261}$$

According to Thome et al., studies range of application for evaporation, condensation heat transfer and frictional correlations are shown below:

$3.1 < d_{in} < 21.4$

$0.02 < p_r < 0.8$

$76 < (We/Fr)_L < 884$

Applicable refrigerants: Ammonia, R-11, R-12, R-22, R-32, R-113, R-123, R-125, R-134a, R-236ea, R-32/R-125 near azeotrope, R-402A, R-404A, R-407C, R-410A,
R-502, propane, n-butane, iso-butane and propylene.

2.5.2.7.3.3 Two phase condensation frictional pressure drop

Condensation pressure drop calculations, are shown below as Souza et al. [47] correlations. This method is based on the calculation of the liquid refrigerant pressure drop correlated according to the two-phase section.

$$\Delta P_f = \Delta P_{f,L} {\emptyset_{liq}}^2 \tag{2.262}$$

Where ΔP_f is the frictional pressure drop in liquid phase and ${\emptyset_{liq}}^2$ is the two phase correction factor.

$$\emptyset_{liq}{}^2 = 1.376 + \frac{C_1}{X_{tt}{}^{C_2}} \tag{2.263}$$

Where

If $Fr_L \geq 0.7$

$$C_1 = 7.242 \tag{2.264}$$

$$C_2 = 1.655 \tag{2.265}$$

If $Fr_L < 0.7$

$$C_1 = 4.172 + 5.48Fr_L - 1.564Fr_L{}^2 \tag{2.266}$$

$$C_2 = 1.773 - 0.169Fr_L \tag{2.267}$$

$$Fr_L = \frac{G_{ref}{}^2}{\rho_L g d_i} \tag{2.268}$$

$$X_{tt} = \left(\frac{\rho_V}{\rho_L}\right)^{0.5} \left(\frac{\mu_V}{\mu_L}\right)^{0.125} \left(\frac{1 - x_{ref}}{x_{ref}}\right)^{0.875} \tag{2.269}$$

Correlation is valid for $x_{ref} \geq 0.17$. If $x_{ref} < 0.17$ interpolation between liquid and two-phase correlations should be used.

2.5.2.8 Heat transfer area

The common equations which are used to calculate heat transfer surface are are listed below according to wavy and plain fins. [48]

Fin spacing

$$F_s = F_p - t_{fin} \tag{2.270}$$

Number of fins

$$N_f = \frac{L_{coil} - F_s}{t_{fin} + F_s} \tag{2.271}$$

Coil height

$$H_{coil} = P_t N_t \tag{2.272}$$

Face area

$$A_{face} = H_{coil} L_{coil} \tag{2.273}$$

Outside tube area

$$A_p = \left(\pi d_o L_{coil} - N_f t_{fin}\right) N N_t \tag{2.274}$$

Total surface area

$$A_o = A_f + A_p \tag{2.275}$$

Plain fin area

$$A_f = 2\left[W_{coil} H_{coil} - \left(\frac{\pi {d_o}^2}{4}\right) N_t\right] N_f L_{coil} + 2 H_{coil} t_{fin} N_f L_{coil} \tag{2.276}$$

Wavy fin area

$$sec\theta = \frac{\sqrt{{x_f}^2 + {P_d}^2}}{x_f} \tag{2.277}$$

$$A_f = 2\left(H_{coil} X_l N sec\theta - N_t N \pi {d_o}^2/4\right) N_{fin} \tag{2.278}$$

Minimum flow area is calculated based on the arrangement type such as

For staggered arrangement

$$2a = (P_t - d_o) - (D_c - d_o)t_{fin}N_f \tag{2.279}$$

$$2b = 2\left(\sqrt{\left[\left(\frac{P_t}{2}\right)^2 + {X_l}^2\right]} - d_o - (D_c - d_o)t_{fin}N_f\right) \tag{2.280}$$

$$A_o = \left[\left(\frac{H_{coil}}{P_t} - 1\right)c + (P_t - d_o) - (d_c - d_o)t_{fin}N_f\right]L_{coil} \tag{2.281}$$

If 2a<2b then c=2b else c=2a

For inline arrangement

$$A_o = \left[(P_t - d_o)L_{coil} - (d_c - d_o)t_{fin}N_f L_{coil}\right]\frac{H_{coil}}{P_t} \tag{2.282}$$

CHAPTER 3

COMPRESSOR CYCLE ALGORITHM

Previously, equipment in vapor compression refrigeration cycle were introduced. Furthermore, the equations and correlations of heat transfer and pressure drop calculations were given for all the equipment in distinct flow types and cases. In this section, an algorithm is proposed which uses all the discussed equations and correlations to connect all the equipment in the refrigeration cycle and documents the effect of all equipment on the cycle as a real time simulation.

In order to specify specific application, the following information is required for the program:

- Outdoor temperature & relative humidity (RH)
- Indoor temperature & RH
- Air flow over condenser and evaporator
- Air flow distribution around the condenser and evaporator copper tubes
- Condenser and evaporator circuit arrangement
- Refrigerant type
- Compressor model
- Compressor sub-cooling and superheat point
- Suction and discharge copper tube diameter, length and settlement
- Compressor cycle mode, cooling or heating

Then, in order for the program to begin iterations ‘calculation button’ should be clicked. Algorithm of the program is given in the figure 3.1. Simulation program first calculates the compressor mass flow. Then, it calculates the discharge tube outlet condensation temperature to use in condenser inlet. Condenser calculations can start with the inlet condensation temperature. In condenser, pressure drop, heat transfer and outlet temperature of refrigerant and air are calculated in each segment. Then, if condenser outlet subcooling value is the same with compressor subcooling value which is a user input, simulation program continues with the next step to calculate liquid line pressure drop and refrigerant mass; otherwise, it iterates

until compressor condensation temperature error decreases to 1°C. After liquid line calculations, program continues with evaporator calculations, which are similar to condenser side. Then, program calculates the suction line outlet evaporation temperature and superheat temperature. If these values are the same same with compressor inlet values calculations, the calculations are stopped and the results are written; otherwise the algorithm iterates to reduce compressor condensation and evaporation temperature until the error decreases to 1 ˚C. Overall, the algorithm uses heat transfer and pressure drop equations and correlations in order to calculate all properties for the entire cycle. The user can also decide to the number of segments the problem to be divided. However, it should be noted that the number of segments increases the accuracy but also computational time. Furthermore, the algorithm calculates the values and iterates until all the properties in the cycle are in accord.

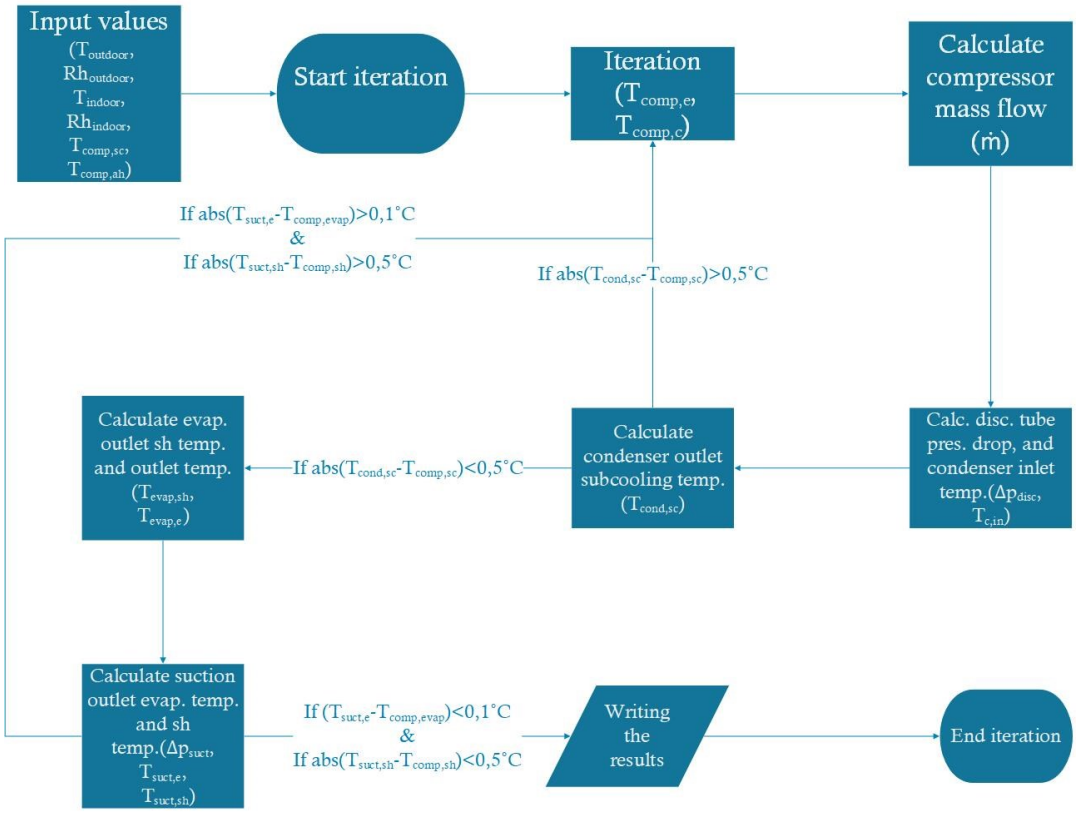

Figure 3-1 Software simulation algorithm

CHAPTER 4

HEAT EXCHANGER SIMULATION RESULTS

Here the results of the developed algorithm is compared with Friterm heat exchanger simulation program. Unfortunately, the cost of experimental study was a constraint so is the lack of experimental data in the literature. Therefore, it is decided to validate the algorithm with commercially used software of Friterm heat exchanger simulation program. The same problem is defined in both software defined as in Tables 4-1 and 4-2. Then, capacity and pressure drop values supplied by the softwares are compared. Main difference between the developed algorithm and Friterm software is related with the circuitry of the exhangers and air flow distribution. Friterm software [49] is not capable of including the circuitry information and it uses common circuitry algorithm of Z shape. In addition, it does not enable user to define air flow distribution and uses uniform air flow distribution in the software. However, developed software enables for user to include the circuitry of heat exchangers and include how the air flow distributed over the exchangers. Especially, if there is a computational fluid dynamics simulations at hand that can be incorporated to enhance to accuracy of the results.

Table 4-1 Condenser calculation comparation between this study and Friterm software (Source: [49])

Condenser Comparison			
		Simulation Programme	Friterm
Tube in rows		2	
Tube number		36	
Length of heat exchanger	mm	800	
Copper tube wall thickness	mm	0,4	
Copper tube out diameter	mm	9,52	
Tube distance in rows	mm	22	
Tube distance in columns	mm	25,4	

Number of circuits		6	
Fin thickness	mm	0,12	
Fin spacing	mm	2,1	
Fin type		Wavy	
Refrigerant type		R410A	
Condensation temp	˚C	55	
Condenser inlet temperature	˚C	95,19	
Refrigerant mass flow	kg/h	392	
Air flow	m^3/h	7800	
Air inlet temperature	˚C	35	
Air inlet RH	%	40,29	
Segments in each tube		5	-
Total capacity	kW	21,12	21,8
Air outlet temperature	˚C	43,2	43,7
Air outlet RH	%	25,9	26,2
Refrigerant side pressure drop	kPa	8,53	10,7
Outlet condensation temperature	˚C	54,8	-
Outlet subcooling	˚C	2,4	5
Refrigerant mass	kg	1,33	-

Table 4-2 Evaporator calculation comparation between this study and Friterm software (Source: [49])

Evaporator Comparison			
		Simulation Programme	Friterm
Tube in rows		3	
Tube number		36	
Length of heat exchanger	mm	500	
Copper tube wall thickness	mm	0,4	
Copper tube out diameter	mm	9,52	
Tube distance in rows	mm	22	

Tube distance in columns	mm	25,4	
Number of circuits		6	
Fin thickness	mm	0,12	
Fin spacing	mm	2,1	
Fin type		Wavy	
Refrigerant type		R410A	
Condensation temp	˚C	55	
Evaporation temp	˚C	7	
Condenser subcooling	˚C	5	
Refrigerant mass flow	kg/h	410	
Air flow	m^3/h	3600	
Air inlet temperature	˚C	27	
Air inlet RH	%	46,94	
Segments in each tube		5	-
Total capacity	kW	17,28	16,8
Sensible heat ratio	%	0,71	0,8
Air outlet temperature	˚C	16,9	15,7
Air outlet RH	%	74,2	83,41
Refrigerant side pressure drop	kPa	28,3	27,8
Outlet evaporation temperature	˚C	6,12	-
Outlet superheat	˚C	12,71	8
Refrigerant mass	kg	0,47	-

CHAPTER 5

CONCLUSION

In this study, basic equipment of water-cooled and air-cooled vapor compression cycle were introduced. The equipment was specified and the advantages and disadvantages of specific type of equipment were discusses such as piston, screw and rotary compressors. The heat transfer and pressure drop equations were given for finned tube heat exchangers specifically for condensers and evaporators. The correlations were specified whether the flow is single phase or two phase, if two phase what is the characteristics of the flow (slug, intermittent or annular zone) and Reynolds number. The mathematical calculation model of zone-by-zone, tube-by-tube and segment by segment were specified. Each method calculates the correlations for defined zones, tubes or segments. Segment by segment method is selected for the developed algorithm because it is the most accurate method if the segment number is increased. In addition, its results can be adopted that if the segment number is the same with the number of tubes then the results became the same with the tube by tube method. After introducing the correlations and deciding on the mathematical calculation method, difference between e-Ntu and LMTD are discussed. Then, the compressor polynomials were documented. The algorithm of the developed software was also discussed where not only a specific heat exchanger calculated by the software but the all the properties for all components are calculated simultaneously. Therefore, the designer should not use several selections software packages, one for condenser, another for evaporator and so on. In addition, as the design parameters varied the input values for each program should be altered and working conditions should be satisfied by the user. However, developed software eliminates this confusion by enabling all the simulations to be run simultaneously and satisfy working conditions automatically. Then in order to validate the accuracy of the developed software, the results of a commercially available heat exchanger selection software was used. The results of the sample case showed that the results of the developed software is acceptable.

REFERENCES

[1] "https://www.nist.gov/services-resources/software/evap-cond," NIST. [Online].

[2] "https://sourceforge.net/projects/achp/," [Online].

[3] "https://iklimsoft.com/," İklimsoft. [Online].

[4] "https://ww2.arb.ca.gov/resources/documents/high-gwp-refrigerants," State of California, 2019. [Online].

[5] T. M. Harms, E. A. Groll and J. Braun, "Accurate charge inventory modeling for unitary air conditioners," 2003.

[6] F. Ragazzi and C. Pedersen, "Modular based computer simulation of an air cooled condenser," Air Conditioning and Refrigeration Center. College of Engineering. University of Illinois at Urbana-Champaign., 1991.

[7] S. Y. Liang, T. N. Wong and Nanyang, "Study of refrigerant circuitry of evaporator coils with a distrubuted simulation model," in *International Refrigeration and Air Conditioning Conference*, 1998.

[8] P. A. Domanski and D. Yashar, "An optimized design of finned tube evaporators using the learnable evolution model," *HVAC&R RESEARCH Vol:10,* pp. 201-211, 2004.

[9] "https://www.indiamart.com/proddetail/finned-tube-heat-exchanger-11661454891.html," IndiaMART InterMESH Ltd.. [Online].

[10] "http://www.hjaluminium.com/aluminium-profile/aluminium-tube/microchannel-heat-exchanger.html," Hongji Aliminium. [Online].

[11] "http://www.thermofin.net/products/caleos-shell-and-tube-heat-exchangers/," Thermofin. [Online].

[12] "https://www.alfalaval.com/microsites/gphe/types/," Alfa Laval. [Online].

[13] "https://www.alfalaval.com/products/heat-transfer/plate-heat-exchangers/brazed-plate-heat-exchangers/cb/," Alfa Laval. [Online].

[14] Emerson. [Online]. Available: https://climate.emerson.com/documents/zp-r410a-scroll-compressors-range-en-gb-4763438.pdf.

[15] Frascold. [Online]. Available: https://www.frascold.it/public/files/files/FCAT250_02_EN.pdf.

[16] "http://www.trainingsystemsaustralia.com.au/products/electrical-engineering-electro-technologies/refrigeration-and-air-conditioning/cutaways/semi-hermetic-compressor-cutaway/," [Online].

[17] "https://www.imagenesmy.com/imagenes/scroll-compressor-icon-d9.html," [Online].

[18] "https://www.frascold.it/en/blog/evento/ahr_expo_2017_las_vegas," Frascold. [Online].

[19] "https://www.danfoss.com/en/products/filters-sight-glasses-and-switches/dcs/filter-driers/dmt-hermetic-filter-driers-for-co2/," Danfoss. [Online].

[20] "http://www.sanhehvac.com/Liquid-Receiver.html," [Online].

[21] "https://hvactutorial.wordpress.com/sectioned-components/suction-accumulator/," [Online].

[22] "https://store.danfoss.com/en/Shut-off-ball-valve%2C-Type%3A-GBC-42s-H/p/009L7411," Danfoss. [Online].

[23] ARI, "Forced-circulation air-cooling and air-heating coils, ARI standard 410.," Air-conditioning and refrigeration institute, Virginia, 2001.

[24] C. E. Mullen, B. Bridges D., K. Porter and G. a. B. Hahn, "Development and validation of a room air conditioning simulation model," in *ASHRAE transactions*, 1998.

[25] H. Jiang, A. Vikrant and R. Radermacher, "CoilDesigner: a general-purpose simulation and design tool for air-to-refrigerant heat exchangers," 2006.

[26] F. P. Incorpera, D. P.Dewitt, T. L. Bergman and A. S. Lavine, "Heat Exchangers," in *Fundementals of heat and mass transfer*, Daniel Sayre, 2006, pp. 686-706.

[27] F. a. P. McQuiston, "Heating, Ventilating, and Air-conditioning,4th ed. Chapter 14," 1994, p. 571.

[28] T. Schmidt, "Heat transfer calculations for extended surfaces," 1949.

[29] C. Wang, "Recent progress on the air side performance of fin and tube heat exchangers," *International Journal of Heat Exchangers Vol 1,* pp. 57-84, 2000.

[30] C. Wang, Y. Hsieh and Y. Lin, "Performance of plate finned tube heat exchangers under dehumidifying conditions," *Journal of Heat Transfer Vol. 119,* pp. 109-117, 1997.

[31] W. Pirompugd and S. W. C.C. Wang, "Finite circular fin method for wavy fin and tube heat exchangers under fully and partially wet surface conditions," *International journal of heat and mass transfer,* pp. 1-16, 2008.

[32] W. Pirompugd, C. C. Wang and S. Wongwises, "Finite circular fin method for wavy fin-and-tube heat exchangers under fully and partially wet surface conditions," *International Journal of Heat and Mass Transfer,* pp. 4002-4017, 2008.

[33] W. Pirompugd and S. W. C.C. Wang, "The new mathematical models for plain fin and tube heat exchangers with dehumidification," *ASME Journal of Heat Transfer Vol.137,* pp. 1-11, 2015.

[34] C. Wang and Y. L. Y.M. Hwang, "Empirical correlations for heat transfer and flow friction characteristics of herringbone wavy fin and tube heat exchangers," *International journal of refrigeration Vol 25,* pp. 673-680, 2002.

[35] C. Wang, Y. Du, Y.J.Chang and W. Tao, "Airside Performance of Herringbone Fin-and-Tube Heat," *THE CANADIAN JOURNAL OF CHEMICAL ENGINEERING, VOL 77,* pp. 1225-1230, 1999.

[36] W. Pirompugd and S. Wongwises, "Actual dry-bulb temperature and equivalent dry-bulb temperature methods for wavy fin-and-tube heat exchangers with dehumidification," *International Journal of Heat and Mass Transfer Vol 106,* pp. 675-685, 2016.

[37] W. Pirompugd and S. W. C.C. Wang, "A review on reduction method for heat and mass transfer characteristics of fin and tube heat exchangers under dehumidifying conditions," *International Journal of Heat and Mass Transfer Vol 52,* pp. 2370-2378, 2009 .

[38] C. Wang, Y. Lin and C. Lee, "Heat and momentum transfer for compact louvered fin and tube heat exchangers in wet conditions," *International journal of heat and mass Transfer Vol 43,* pp. 3443-3452, 1999.

[39] C. Wang, W. Lee, W. Sheu and Y.-J. Chang, "Parametric study of the air ide performance of slit fin and tube heat exchangers in wet conditions," *Proc Instn Mech Engrs Vol 215,* pp. 1111-1121, 2001.

[40] J. Thome, J. Hajal and A. Cavallini, "Condensation in horizontal tubes, part 1: two

phase flow pattern map," *International Journal of Heat and Mass Transfer Vol:46,* pp. 3349-3363, 2003.

[41] J. Thome, J. Hajal and A. Cavallini, "Condensation in horizontal tubes, part 2: new heat transfer model based on flow regimes," *International journal of heat and mass transfer,* pp. 3365-3387, 2003.

[42] J. Thome and T. U. L. Wotjan, "Investigation of flow boiling in horizontal tubes: Part I A new diabatic two-phase flow pattern map," *International heat and mass transfer Vol:48,* pp. 2955-2969, 2005.

[43] J. Thome and T. U. L. Wotjan, "Investigation of flow boiling in horizontal tubes: Part II Development of a new heat transfer model for stratified-wavy, dryout and mist flow regimes," *International jurnal of heat and mass transfer Vol:48,* pp. 2970-2985, 2005.

[44] V. Gnielinski, "New equation for heat and mass transfer in turbulent pipe and channel flow," *Int. Chem. Eng. Vol: 16,* pp. 359-368, 1976.

[45] S. Zivi, "Estimation of steady state steam void fraction by means of the principle minimum entropy production," *ASME Journal of heat transfer,* pp. 247-251, 1964.

[46] J. Thome and J. Quiben, "Flow pattern based two-phase frictional pressure drop model for horizontal tubes. Part I: Diabatic and adiabatic experimental study," *International journal of heat and fluid flow Vol:28,* pp. 1049-1059, 2007.

[47] A. L. Souza, J. C. Chato, J. M. S. Jabardo, J. P. Wattelet, J. Panek, B. Christoffersen and N. Rhines, "Pressure drop during two-phase flow of refrigerants in horizontal smooth tubes," Air Conditioning and Refrigeration Center. College of Engineering. University of Illinois at Urbana-Champaign., 1992.

[48] R. K. Shah and D. P. Sekulic, Fundemantals of heat exchanger design, 2003.

[49] F. A.Ş., "Friterm," 2016. [Online]. Available: https://www.friterm.com/tr-TR/isi-esanjorleri-tasarim-programi-friterm-frtcoils/13022.

[50] S. Kakac, "Heat Transfer Enhancement of Heat Exchangers," 2002, pp. 141-162.

[51] C. C. Wang, "On the airside performance of fin and tube heat exchangers," in *Heat Transfer Enhancement of Heat Exchangers*, 1999, pp. 141-162.

[52] J. Thome and J. Quiben, "Flow pattern based two-phase frictional pressure drop model

for horizontal tubes, Part II: New phenomenological model," *International journal of heat and fluid flow Vol:28,* pp. 1060-1072, 2007.

[53] S. Fischer, C. Rice ve W. Jackson, «The Oak ridge heatpump design model: Mark III version program documentation,» Oak Ridge Natioanal Laborotory, 1988.

[54] C. Mullen, B. Bridges, K. Porter, G. Hahn ve C. Bullard, «Development and validation of a room air conditioning simulation model,» 1997.

[55] P. A. Domanski and D. Didion, "Computer Modeling of the Vapor compression cycle with constant flow are expansion device," vol. 155, 1983.